Inorganic Chemistry, Vol. 17, No. 9, 1978 **2537**

Contribution from the Department of Chemistry,
Cornell University, Ithaca, New York 14853

A Molecular Orbital Approach to Electron-Transfer Reactions between Transition-Metal Ions in Solution

JEREMY K. BURDETT[1]

Received July 13, 1977

We present a general scheme to rationalize the kinetic behavior of transition-metal redox systems in solution as a function of the detailed electronic configurations of donor and acceptor species. For the inner-sphere route, proceeding usually via atom transfer, simple molecular orbital arguments are used to predict for which electronic configurations L_5M_1–X–M_2L_5 complexes will be stable at the symmetric geometry. The results are supported by comparison with known crystal structures. For these electronic configurations then the symmetric structure corresponds to an inner-sphere intermediate, sometimes observed spectroscopically or inferred kinetically in the experimental environment. For other configurations the symmetric structure corresponds to a transition state which is never observed experimentally. The kinetic behavior of a large number of redox systems may be rationalized just on this basis. It is suggested that the normal dependence of reaction rate on bridging ligand X ($I^- > Br^- > Cl^- > F^-$) arises when the rate-determining step involves a transition state (we call this type I) and the inverse order when the rate-determining step involves intermediate decay (type II). The dependence of reaction rate upon substituent in some carboxylate-bridged systems is also examined, and the effects of nonbridging ligands are analyzed by extending earlier ideas of Orgel. Two types of electron transfer are delineated. Smooth transfer occurs when the nature of the HOMO gradually changes as the bridge ligand is transferred and corresponds to a symmetry-allowed process. Sudden transfer occurs via an electron jump from one orbital to another, and atom transfer here is not necessary for electron transfer. Cases are observed experimentally where atom transfer does not occur. The results of the inner-sphere case are applied to outer-sphere reactions with some qualifications, and some interesting parallels are drawn. The effect of extra ions added to the solution are analyzed in molecular orbital terms, and three catalytic effects are revealed. The added species may hold together the two reacting ions as an electrostatic "glue" (if of the correct charge); it may reduce the barrier to reaction and also may ensure adiabatic behavior. It is pointed out that water itself is probably an excellent catalyst of this sort. The molecular orbital approach to inner- and outer-sphere reactions gives a ready explanation for the anomalous behavior (on the Marcus theory) of the $Co^{II,III}(H_2O)_6$ system where a spin change occurs in the reaction coordinate.

Introduction

The oxidation and reduction reactions of transition-metal ions in aqueous solution have long received a large share of experimental and theoretical study in the field of reaction kinetics. Several excellent reviews and monographs[2] lay out the present state of the art in both areas. Theoretical considerations to date have been dominated by the Franck–Condon principle which only allows the electron-transfer event to occur without a change in nuclear configurational parameters. Thus, reductant and oxidant need to rearrange and find some "common state" where the electron may be transferred without nuclear rearrangement. The energy needed to attain this common state includes ligand field, solvation, and electrostatic terms. The parameterization of these contributions has formed the basis of the approaches of Marcus, Hush, and others[3] which attempt to rationalize the rates of these reactions.

Two distinct modes of reaction have been identified experimentally for these simple redox reactions, largely through the early work of Taube and his collaborators. The *outer-sphere* reaction is one in which the ligands bound directly to the metal atoms remain intact (although not undisturbed) during the course of the reaction. Since a largely metal-located d-orbital electron usually lying in a metal–ligand antibonding orbital is transferred from one ion to another, the M–L bond in the oxidized species contracts and that in the reduced species expands.[4] Application of the Franck–Condon principle demands that some of this bond extension and compression occur before electron transfer to equate the energies of donor and acceptor sites. Thus, in Figure 1 we see how the Fe^{III}–O bond is stretched and the Fe^{II}–O bond compressed to arrive at the point × where electron transfer may occur for Fe^{II}/Fe^{III} exchange.[6] Ab initio molecular orbital calculations designed to calculate these two energy changes for this system have recently been performed.[7] Since the metal t_{2g} orbital set of the octahedral complex is less M–L antibonding than the e_g set, the energy changes needed to reach the activated complex for $t_{2g} \rightarrow t_{2g}$ transfer should be smaller than those associated with $e_g \rightarrow e_g$ transfer. Ideas similar to these have been extensively used to rationalize the faster rates of the former type of electron transfer.

In general, where the donor and acceptor sites are coupled electronically, the two curves representing reactant and product energies will repel each other (Figure 2). $\Delta\epsilon$ is twice the so-called resonance energy and is a measure of the coupling between the two metal centers. If $\Delta\epsilon$ is large, then the electron-transfer process is adiabatic and the rate of reaction can be understood in terms of passage over an activation barrier. If $\Delta\epsilon$ is small, then nonadiabatic behavior results where the electron-transfer probability is less than unity on passing through the funnel. The rate of reaction then involves the Landau–Zener formulation governing the rate of passage from reactant curve to product curve. Most electron-transfer reactions are probably of the adiabatic type. (See ref 2h for a discussion.)

The *inner-sphere* reaction occurs via formation of a bridged species after one of the reactants (usually the reductant) has lost a coordinated ligand. The vast majority of the redox processes we shall discuss here involve hexacoordinated ions[8] and thus the geometry of the bridged intermediate or transition state resembles **1**. In many cases a bridged intermediate has

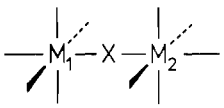

1

been spectroscopically detected in solution, or its presence inferred kinetically from the form of the rate law. Many related species are available in crystal structures amenable to X-ray characterization. Several of these are mixed-valence molecules where there is a lot of current interest in the factors influencing the rate of electron transfer between the two metal sites. In the solution environment electron transfer is suggested to occur within the bridged species, and in the majority of cases this is accompanied by atom transfer—usually the bridging

0020-1669/78/1317-2537$01.00/0

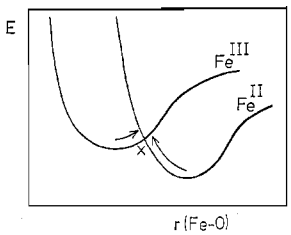

Figure 1. Energy changes associated with changes in Fe–O bond lengths in $Fe^{II,III}(H_2O)_6^{2+,3+}$. At the point × the energies of the Fe^{II} and Fe^{III} sites are equal. The arrows represent the two reorganizational energies needed to achieve this "common state".

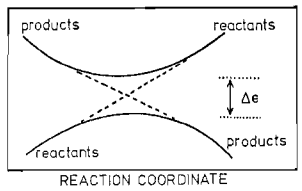

Figure 2. General energy scheme for electron transfer. The resonance energy is $\Delta\epsilon/2$.

atom or group is transferred from oxidant to reductant.

Halpern and Orgel[9] have delineated four distinct processes for electron transfer: (i) direct transfer via overlap of a d orbital on one center with a d orbital on the other, this probably being of secondary importance in these systems due to the relatively large metal–metal separation; (ii) double exchange with simultaneous electron transfer from one metal atom to the bridge and from the bridge to the second metal atom; (iii) the chemical mechanism (eq 1) where the electron actually

$$M^nXM^{m+1} \rightarrow M^{n+1}\text{–}X^-\text{–}M^{m+1} \rightarrow M^{n+1}\text{–}X\text{–}M^m \quad (1)$$

reduces the bridging group, this being ruled out[10] on thermodynamic grounds for most inorganic bridges but remaining a possible mechanism for some organic bridges; (iv) the superexchange mechanism also used to account for the magnetic interaction between transition metal ions.

A general scheme for the inner-sphere redox process is shown in **2**. We shall sometimes need to modify this scheme

$$M_1{}^nB_6 \xrightarrow[\text{ligand loss}]{k_1} M_1{}^nB_5$$

$$M_1{}^nB_5 + M_2{}^{m+1}A_5X \xrightarrow[\text{precursor complex}]{k_2} B_5M_1{}^n\text{–}X\text{–}M_2A_5{}^{m+1}$$

$$B_5M_1{}^n\text{–}X\text{–}M_2{}^{m+1}A_5 \xrightarrow[\text{electron transfer}]{k_3} B_5M_1{}^{n+1}\text{–}X\text{–}M_2{}^mA_5$$

$$B_5M_1{}^{n+1}\text{–}X\text{–}M_2{}^mA_5 \xrightarrow{k_4} B_5M_1{}^{n+1}X + M_2{}^mA_5$$

2

in the light of our discussion below, but the general picture is a useful starting point. A large amount of experimental effort has been expended in deciding which route, inner or outer sphere, or the relative contributions of each, is followed for a particular redox system. There is an excellent summary of the experimental methods of attack in Wilkins' book.[2c]

Obviously those systems which are going to give us most information about the electron-transfer process are those where the rate-determining steps in the scheme **2** are associated with the electron-transfer step(s). Thus reductions by V^{II} although potentially very interesting are often found to have similar rate constants independent of the nature of the oxidant. This is ascribed to the fact that five-coordinate formation is the rate-determining step (k_1 of scheme **2**) and means that we glean little information about the inner-sphere route in this case. We shall be mostly concerned with reactions where the rate-determining steps appear later in the reaction sequence.

Molecular orbital arguments have not in general been used to describe these reactions[11] with the exception of some particularly perceptive comments by Orgel[12] over 20 years ago which have been neglected for the most part over the intervening years. The purpose of this work is to fill such a theoretical gap and provide a unified approach to the intimate mechanism of transition-metal redox behavior.

In contrast to a bridged species, well documented by inference or actual detection for the inner-sphere route, virtually no information is available concerning the nature of the outer-sphere transition state. Our molecular orbital deliberations will then lie mainly with the details of the inner-sphere process, although, as we shall see later, many of the concepts and results carry over directly into the outer-sphere case after we make some geometrical assumptions. We shall use extended Hückel molecular orbital calculations on simple model systems (see Appendix) to aid us in this task but caution the reader that the results obtained using this semiempirical method are best regarded in a qualitative light and this is precisely how we shall usually view them. Orbital symmetry and overlap arguments will form the basis of our approach.

Molecular Orbital Structure of Inner-Sphere Intermediate or Transition State

Let us initially look at the molecular orbital structure of a symmetrically bridged species **1**. In all of these redox systems it is going to be very important to have a detailed knowledge of the electronic structure of a molecular geometry which may correspond to an intermediate or transition state. It is instructive to build this up from two C_{4v} square-pyramidal ML_5 units[13] as in Figure 3. The frontier region of the ML_5 unit consists (Figure 3a) of a set of three d orbitals at low energy (b_1, e) derived from the t_{2g} orbitals of the octahedron. To higher energy lie the orbitals derived from the e_g set. The a_1 orbital [nd_{z^2} mixed with $(n+1)$s, p_z orbitals] is well shaped to interact with another ML_5 unit located along the z axis. The $x^2 - y^2$ orbital to higher energy is located in the xy plane and poorly located for such interactions. Thus the only significant orbital splittings are for the in- and out-of-phase arrangements of the z^2 orbitals on each ML_5 unit (Figure 3b).

A large number of ligands have been used as bridging groups.[14] For illustrative purposes in Figure 3c we have shown the effect of using a single halogen bridge. For most bridging ligands the overall pattern will be very similar, although a trivial reversal of the ordering of the levels σ_g and σ_u (using symmetry labels appropriate to the $D_{\infty h}$ point group of the M_1XM_2 unit) may occur in some instances. The four mainly ligand located orbitals to low energy are always completely filled, and the stabilization energy afforded these orbitals represents the binding energy of the M_1XM_2 complex. The lowest energy metal d orbitals are of π type. π_g has no ligand counterpart; π_u is involved in antibonding M–X interaction and the in- and out-of-phase combinations of the xy orbitals are approximately equienergetic and contain no X character. The largest interactions are to higher energy and are the σ interactions of the linear M_1–X–M_2 bridge. Which orbital of σ_g, σ_u lies to higher energy depends on the nature of X. Their relative ordering, however, does not influence our arguments presented below concerning the stability of this structure. At the very top of the diagram lie the δ-type orbitals formed by in- and out-of-phase combinations of $x^2 - y^2$ on the two centers. They are approximately equienergetic. Some of the features of this molecular orbital diagram were elucidated[15] by Dunitz and Orgel and more recently by others. With a bridging H atom the diagram of Figure 3 will be slightly different in that the σ_u orbital remains unchanged in energy on moving from Figure 3b to Figure 3c, simply due

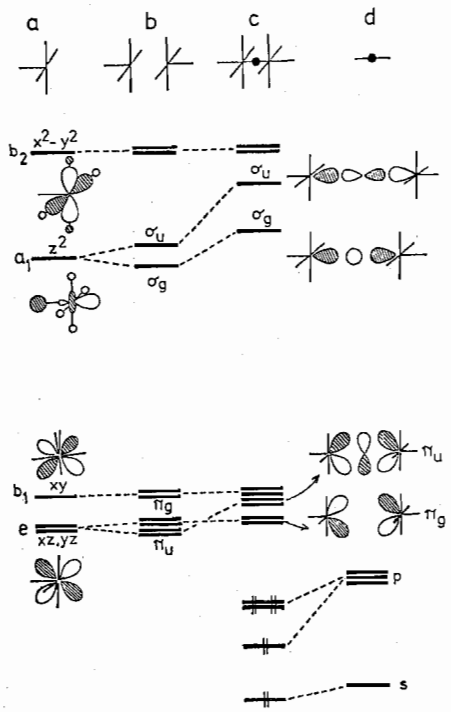

Figure 3. Molecular orbital diagram for a symmetrically bridged M_2X_{11} species (c) assembled via a symmetric M_2X_{10} unit (b), from a bridging atom (d) and square-pyramidal MX_5 unit (a). The diagram is to be regarded schematically and is not to scale. The σ, π labels refer to the orbital symmetry under the $D_{\infty h}$ point group of the MXM unit.

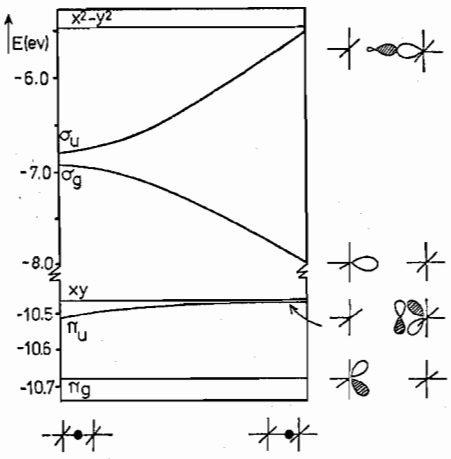

Figure 4. Orbital energies of $Cr_2Cl_{11}^{6-}$ as a function of bridging atom asymmetrization. The labels xy and $x^2 - y^2$ refer to in-phase/out-of-phase pairs of orbitals of this type which are essentially equienergetic. Note the broken energy scale separating "e_g" and "t_{2g}" type orbitals and also that the halves of the diagram are on different scales. The labels σ, π refer to the orbital symmetry under the $D_{\infty h}$ point group of the MXM unit.

to the lack of an accessible 2p orbital on the H atom.

We show the geometrical change associated with the inner-sphere process on atom transfer in **3**. Let us see how the

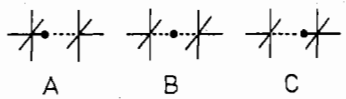

3

energies of the molecular orbitals change as the bridge is made asymmetric, i.e. B → A, C. Quantitative energy changes are shown in Figure 4. First, our calculations on model systems show that the system with no d electrons is most stable at the

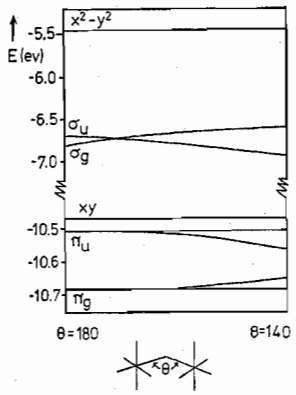

Figure 5. Orbital energies of $Cr_2Cl_{11}^{6-}$ as a function of bending around the bridging Cl atom. The labels xy and $x^2 - y^2$ refer to in-phase/out-of-phase pairs of orbitals of this type which are essentially equienergetic. Note the broken energy scale separating "e_g" and "t_{2g}" type orbitals and also that the halves of the diagram are on different scales. The labels σ, π refer to the orbital symmetry under the $D_{\infty h}$ point group of the MXM unit.

symmetric geometry, but the energy change associated with asymmetrization is small. We can therefore focus on the energy changes within the d-orbital manifold alone when viewing other electronic configurations. The π_u orbital is destabilized for the X = halogen models we have examined. A more repulsive interaction is felt with one short and one long MX distance than two average MX distances.[16] The lower energy σ orbital is dramatically stabilized since now this orbital corresponds to z^2 on one five-coordinate unit. The higher energy σ orbital is destabilized since this orbital now corresponds to a z^2 orbital on the six-coordinate unit. The σ_g and σ_u orbitals mix together strongly under the asymmetrization perturbation, and this leads to a strong mutual repulsion. This coupling together of z^2 orbitals on the two metal centers by the bridging group, responsible for the increase in splitting between σ_g and σ_u on moving from b to c in Figure 3 has been called[17] "through-bond coupling" by Hoffmann.

Another degree of freedom possessed by the symmetric structure is that of bending about the central atom. For the species with no d electrons this is a costly business for our halogen model systems. We show the energy changes within the d-orbital manifold in Figure 5. On bending, the σ_g and σ_u orbitals mix with components derived from the π_u and π_g orbitals, respectively.[17b] The largest energy changes occur in the σ manifold, but even so the magnitudes are smaller than those involved in the asymmetrization process of Figure 4. A similar diagram holds for the related distortion where the M_2X_{10} part of the molecule is held fixed and the bridging ligand set off axis. For the case where the bridging ligand is a hydrogen atom, then the σ_u orbital and both components of the π_g orbital remain approximately equienergetic in either distortion mode, because of the absence of an accessible p-type orbital on the H atom.

Structures of Monobridged Dimers

We may use the ideas of the previous section to understand the gross structural features of systems of this type, containing an MXM skeleton as a function of the number of metal d electrons. This will be of vital importance to us later, since we shall need to be able to predict whether a transition state or intermediate corresponds to the symmetric geometry for a given electronic configuration. A detailed discussion of the structural preferences of all possible electron configurations would be lengthy and so we select some of interest and compare theoretical predictions with experiment. We shall use a dual notation to describe the electron configurations of these systems. First, we shall describe the configurations of the two reactants as $d^n d^m$. Thus a Cr^{II}/Cr^{III} system is de-

scribed as hsd^4hsd^3 and Fe^{II}/Co^{III} as hsd^6lsd^6 (hs, ls = high spin, low spin). Second, we shall describe occupancy of the binuclear species as $\pi^n\sigma_u^m\sigma_g^l$ where we specify the number of electrons in the six lowest lying π-type (with respect to the octahedral geometry) d orbitals and the two higher energy σ orbitals.

For all systems with the π^n configuration (n = 0–12) the symmetric structure is predicted to be most stable. This is observed for the d^0d^0,π^0 species $Nb_2F_{11}^-$ where a distorted but approximately symmetric geometry is seen.[18] Similarly the NbF_5 structure (**4**) found[18] for the d^0 and d^1 pentafluorides

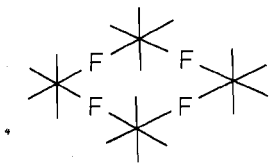

4

of Nb, Ta, Mo, and W consists of symmetrically bridged tetrameric units. For the RuF_5 structure, found[18] for the pentafluorides of Ru, Os, Ir, Rh, and Pt, a symmetrically bridged tetramer is found with MFM angles of ~130°. (The RuF_5 binuclear complex would have the configuration hsd^3hsd^3, π^6.)

A linear, near-symmetric structure is found for an analogue[19] of ruthenium red (**5**). The oxidation states of the

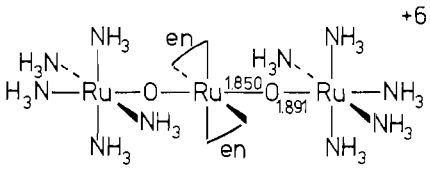

5

Ru atoms are suggested to be II, VI, and II leading to a $lsd^6hsd^2lsd^6$ structure where all the electrons reside in the metal π manifold. For the hsd^3hsd^3, π^6 structure we have the oxo- and hydroxy-bridged chromium(III) species[20] (**6**). The former

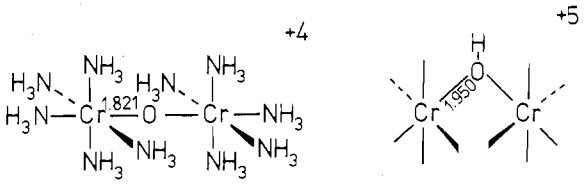

6

are linear symmetric species; the latter, symmetric but bent about the central O atom due to the presence of the H atom. A related species with the same electronic configuration and a structure[21] identical with that of the Cr^{III}–oxo dimer is $Re_2Cl_{10}O^{4-}$. Species with the lsd^4lsd^4 configuration are represented by symmetric, linear $Mn_2(CN)_{10}O^{6-}$,[22] $Ru_2Cl_{10}O^{4-}$,[23] and $Ru_2(H_2O)_2Cl_8N^{3-}$[24] species. We are not aware of any lsd^5lsd^5, π^{10} systems available as crystal structures, but there are plenty of lsd^6lsd^6, π^{12} molecules. $Mn_2(CO)_{10}SnX_2$ (X = Br, I) contains[25] symmetrically bridged $Mn(CO)_5$ units, bent about the central Sn atom due to the presence of the two halogen atoms. $Co_2(NH_3)_{10}NH_2^{5+}$ has[26] a similar gross structure. Several mixed-valence molecules containing nitrogen-bearing bridges have been spectroscopically identified,[27] but no crystal structures have been determined to date. In each of these cases the ligand field strength is large enough to force all the electrons into the π-orbital manifold. A set of rather unusual structures are observed for the isoelectronic molecules $HCr_2(CO)_{10}^-$, $HW_2(CO)_9NO$, and $HW_2(CO)_8PPh_3NO$ where[28] the bridging hydride group is off-axis (M–M) in every case. The bridges are, however, symmetric when the halves of the molecule are chemically identical. In the isoelectronic $Cr_2(CO)_{10}I^-$ a symmetric[29] but bent structure is found. Thus the observation of the symmetric geometry for these π^n systems is in agreement with our theoretical predictions above. What is not well described is the bent nature of some of these molecules where a single bridging atom is present. Our model calculations with halogen or hydride bridges indicate in all instances that the linear MXM geometry should be most stable.[30] Several molecules with π^n electronic configurations have also been observed spectroscopically in redox solutions. Some relevant to our discussion later are shown in Table I.

Table I

reactants	binuclear species	ref
Cr^{II} and V^{IV}	Cr^{III}–O–V^{III}	57
Cr^{II} and $IrCl_6^{2-}$	Cr^{III}–Cl–Ir^{III}	*a*
Cr^{II} and $Ru^{III}ClL_5$	Cr^{III}–Cl–Ru^{II}	56
$Co(CN)_5^{3-}$ and $IrCl_6^{2-}$	Co^{III}–Cl–Ir^{III}	58
$Co(CN)_5^{3-}$ and $Fe(CN)_6^{3-}$	Co^{III}–NC–Fe^{II}	59

[a] A. G. Sykes and R. N. F. Thorneley, *J. Chem. Soc.*, 232 (1970).

Occupation of the lowest lying σ orbital immediately leads to a strong destabilization of the symmetric geometry, this σ effect overwhelming any preferences from the π^n manifold. Perturbation theory tells us that σ_u and σ_g mix together strongly via this asymmetric distortion, and indeed we may consider the instability of the $\pi^n\sigma_g^1$ configuration at the symmetric geometry to be due to a second-order Jahn–Teller effect. As far as we know, with one exception, no symmetrically bridged species have been observed either crystallographically or spectroscopically with $\pi^n\sigma_g^1$, $\pi^n\sigma_g^2$, or $\pi^n\sigma_g^2\sigma_u^1$ configurations where this geometry is predicted to be unstable. However, we do observe[31] for "CrF_5", which contains a mixture of Cr^{II} and Cr^{III} ions in pseudooctahedral sites, the structure **7**. This, when viewed as a binuclear complex, would

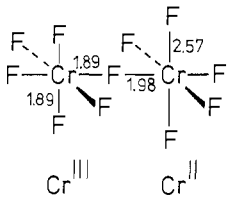

7

have the configuration $\pi^6\sigma_g^1$ arising from hsd^4hsd^3. Interestingly this structure is slightly bent around the bridge fluoride. Figure 5 suggested that with this electronic configuration the symmetric geometry was also unstable to bending. For the $\pi^n\sigma_g^2$ configuration we have the classic series of mixed-valence Pt^{II}/Pt^{IV} molecules (lsd^8lsd^6) which are related to the present story.[32] Here we reproduce the structure of one (**8**) where we see 6 + 4 coordinated structures instead

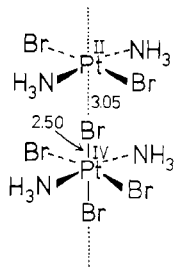

8

of the 6 + 5 pair that we have been discussing above. (The molecular orbital structure of the square-planar fragment will be similar to that of the square-based pyramid in the d-orbital region except that the z^2 orbital will be lower in energy and therefore further away from the $x^2 - y^2$ orbital.) Another

example of the $\pi^n\sigma_g^1$ configuration is presented[34] by Prussian blue (**9**) which consists essentially of $KFe^{III}Fe^{II}(CN)_6$ with a

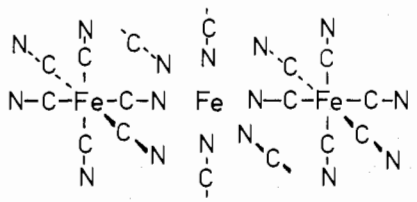

9

high-spin "$Fe^{III}(NC)_6$" environment and low-spin $Fe^{II}(CN)_6$ environment (hsd^5lsd^6). The high-spin Fe^{III} has one electron in σ_g and one in $x^2 - y^2$ located on the Fe^{III}.

All three of these examples are what are known as class II mixed-valence species after the classification of Robin and Day.[31] Here the "valencies" are trapped and we can distinctly observe Pt^{II} and Pt^{IV} sites for example. In class IIIA mixed-valence species the electron is delocalized over both centers and they appear to be crystallographically identical. There the electron may be "hopping" back and forth very rapidly. Achievement of the symmetrical structure is probably a necessary condition for occurrence of a class IIIA mixed-valence species where the electron has a chance of being delocalized. Thus we may understand why this behavior is often observed with the π^n complexes noted above, but not with these other systems where the symmetric geometry is unstable. An understanding, in simple molecular orbital terms, of when a given π^n system will exhibit class IIIA or class II behavior is much more difficult to achieve.

With equal occupancy of σ_g and σ_u the slopes of Figure 4 suggest that the symmetric structure can again become a possibility. With the occupation of metal–ligand σ antibonding orbitals we may expect to see rather long bond lengths between the metal and bridging ligands. Both of these effects are seen. In the $(hfac)_2Cu^{II}$ complex[35] of pyrazine (d^9d^9,$\pi^{12}\sigma_g^2\sigma_u^2$) (**10**),

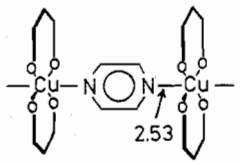

10

with its symmetrically but weakly bound bridging ligand, a more usual Cu–N bond length would be about 1.95 Å. With these symmetric structures class IIIA mixed-valence behavior is possible and indeed much discussion[35] has centered around **10** and related systems. A series of Fe^{III} porphyrin molecules with a bridging O atom $[Fe(porp)]_2O$ have also been structurally characterized.[36] These have symmetrical bridges with the Fe–O distances of ~1.83 Å. They are often bent although linear Fe–O–Fe examples are known. In the series $[Fe(salen)]_2O$·solv the bond angles are about 140° (**11**). The

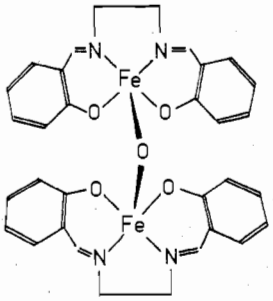

11

molecules are in fact considerably more distorted about each metal atom than we show. These systems are claimed[36a] to be based on high-spin Fe^{III} units (hsd^5hsd^5) which would lead to the $\sigma_g^1\sigma_u^1$ configuration. However the Fe–O bond length does seem rather short. Our molecular orbital diagram of Figure 5 does not anticipate the bent geometry of **11**. Thus, as before, our theory is able to well rationalize the symmetric–asymmetric behavior of these complexes but in general is less able to accommodate the bending of certain structures although these molecules in particular are considerably distorted anyway. The only exception to our theory which we have been able to find is the symmetrically bridged Co^{II} complex (**12**) which is reported[37] to be diamagnetic and thus

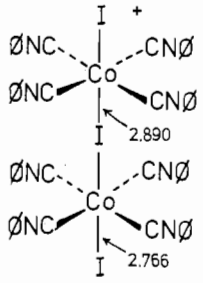

12

has the configuration $\pi^{12}\sigma_g^2$, the same as the platinum examples above. This interestingly points to the area where our simple model, independent of the nature of the transition metal and charge on each metal center, breaks down. In addition to the molecular orbital energy changes of Figure 4 we need to add the variation in energy of the metal levels as the oxidation state of the metal changes. In the present case two Co^{II} units are more stable than a Co^{I} and a Co^{III}, even though the simple molecular orbital arguments of this section, without such modification, argue the opposite. We should bear this point in mind in what follows in the rest of the paper.

In this section then we have combined our new theoretical results with experimental data and defined the conditions under which we expect to observe a transition state or intermediate at the symmetrical bridge geometry. We summarize the results in Figure 6. For the configurations $\pi^n\sigma_g^1$, $\pi^n\sigma_g^2$, and $\pi^n\sigma_g^2\sigma_u^1$ the symmetric geometry corresponds to a transition state, and the reaction profile on atom transfer for a system with one of these configurations is shown at the top of Figure 6. We will call this a type I profile. For any other configuration, namely, π^n, $\pi^n\sigma_g^1\sigma_u^1$, and $\pi^n\sigma_g^2\sigma_u^2$, we should find a stable intermediate. This profile is shown at the bottom of Figure 6 and we will call this a type II profile. For the sake of simplicity we draw the turning points of Figure 6 with equal stabilization/destabilization energies. In fact the type I barrier is expected to be much larger than the type II well, and this is borne out by calculations on model systems. σ effects dominate the type I barrier, but π effects temper the type II well.

Before we look at some experimental results on the kinetics of redox systems however, we need to understand how the electron is transferred within this transition state or intermediate.

The Process of Electron Transfer

(a) Smooth Transfer. Given that an atom or bridging ligand group is invariably transferred some time during the reaction, what is the connection between this motion and the "movement" of the electron? First, let us consider how the natures of the σ-type orbitals change during the process. This is shown in Figure 7 for the $\pi^n\sigma_g^1$ configuration. In A the odd electron is located entirely on the five-coordinate unit, in B it is now shared equally between both metal atoms, and in C it has been transferred to the other metal atom which is now five-coordinate. Thus the electron initially on one metal atom

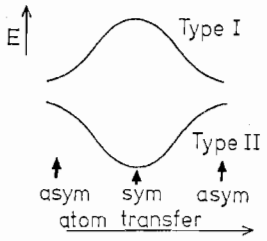

Figure 6. Two types of energy profile associated with bridging group transfer. Type I (for electronic configurations $\pi^n\sigma_g^1$, $\pi^n\sigma_g^2$, and $\pi^n\sigma_g^2\sigma_u^1$) corresponds to a transition state and type II (for electronic configurations π^n, $\pi^n\sigma_g^1\sigma_u^1$, and $\pi^n\sigma_g^2\sigma_u^2$) corresponds to an intermediate at the symmetric geometry. The equal energy changes depicted for both types is for illustrative purposes only. The type I barrier is invariably larger than the type II well (see Figure 4).

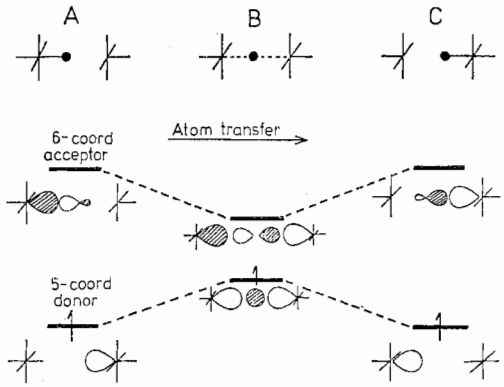

Figure 7. The change in the nature of the σ orbitals of the M_2X_{11} unit as the bridging atom is transferred from the initially six-coordinate acceptor to five-coordinate donor molecule. As the description of the HOMO changes, so the electron is "transferred".

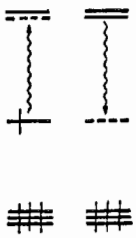

Figure 8. Gross energy changes of z^2 orbitals on donor and acceptor sites as a result of atom transfer.

has been very smoothly transferred from one metal atom to another as a result purely of atom transfer. This result was first pointed out by Orgel.[12] Figure 7 possesses the basic features of the electron-transfer process seen in Figure 2. The resonance energy $^1/_2\Delta\epsilon$ arises from metal–metal overlap and the presence of the bridging ligand which serves to split apart σ_g and σ_u levels. Thus the energy of the z^2 orbital on the five-coordinate unit rises and the energy of the corresponding orbital on the six-coordinate unit decreases (Figure 8) on atom transfer. There is an avoided crossing (Figure 7) at the point where the two would be equienergetic. Smooth electron transfer occurs in this case by passage over a barrier shown in the bottom half of Figure 7 whose height is mediated largely by metal–bridging ligand interactions. We shall use pictorial representations of this transfer similar to **13** extensively below.

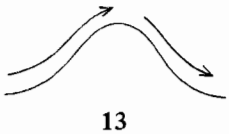

13

Figure 9 shows the result of a calculation on our model

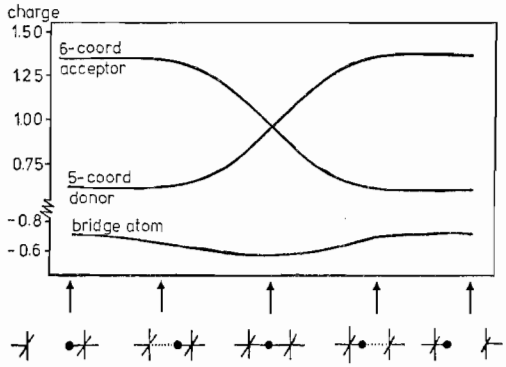

Figure 9. The charges on the two metal atoms and the bridge atom in $Cr_2Cl_{11}^{6-}$ as a function of reaction coordinate. The five- and six-coordinate units are brought from afar to form an asymmetrically bridged unit. The bridging atom is transferred from one metal atom to the other, and the five- and six-coordinate units separate. Note break in scale.

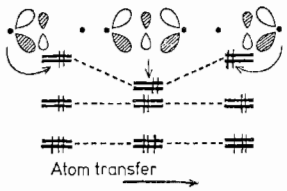

Figure 10. The change in nature of the π-type orbitals on bridging atom transfer. For the case shown an electron is smoothly transferred from the initially five- to initially six-coordinate unit.

chloride-bridged dimer showing how the charge is smoothly transferred from one metal atom to another. No charge builds up on the bridge atom eliminating the chemical mechanism and suggesting that the double-exchange process applies here.

A similar smooth electron transfer between π-type electrons can also be recognized (Figure 10). Here a pair of orbitals change nature as the ligand is exchanged. We show the situation where the highest energy pair of π orbitals are xz, yz on the five- and six-coordinate units. The result is transfer of an electron from the initially six- to the initially five-coordinate unit. The situation here is not as clear-cut as it was in the σ case since here the relative ordering of the π levels will depend on the nature of the other ligands coordinated to the metal atom. The level ordering we show in Figure 10 is different in fact from that found for our model complexes in Figure 3. Only for the situation in Figure 10 will smooth transfer occur on ligand exchange for the electronic configuration shown. Without knowing the detailed arrangement of orbitals in this region it is impossible to map out the "path" of the migrating electron. However with such a density of orbitals configuration interaction may be very important and so talking about molecular orbital effects for a single configuration may not be very meaningful in this particular case. Electron transfer within the π-orbital manifold will then be overall a smooth process, but we will not have to worry about it in molecular orbital terms.

(b) Sudden Electron Transfer. Another way in which electron transfer may occur is via an electron "jump" from one orbital to another while the five- and six-coordinate species are in contact during the tenancy of some sort of bridged species. We may view this sort of electron transfer in an exactly analogous way to the electron jump that occurs when, e.g., Na· and Cl· atoms are brought together to make a Na–Cl molecule. Figure 11 shows the interaction of covalent and ionic curves leading to such a result after the ideas of Mulliken.[38]

In general, in molecular orbital language the location of the electron density in one molecular orbital will be different from that in another and thus an electron jump will result in a

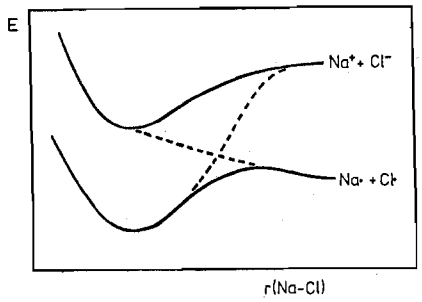

Figure 11. Avoided crossing of "ionic" and "covalent" curves for the formation of sodium chloride from atoms and ions. The electron "jump" occurs in the region containing the dashed lines.

sudden charge redistribution. Conceptually we may envisage such a jump to occur as a result of one or both of two effects. First, the electron may find itself in an orbital of higher energy than an empty one below it somewhere along the reaction coordinate. Second, in response to changes in relevant orbital energies and Racah parameters due to the change in geometry or charge on the metal centers, it may be profitable to promote an electron (s) with a change of spin quantum number such that the energy of the new configuration is lower than that of the old. In the mononuclear complex we are familiar with similar arguments applied to rationalizing the formation of high- and low-spin complexes. We shall find below that there are two instances when sudden electron transfer may occur. First, in reactions where the electron is transferred from an orbital on one metal atom to an orbital on the other metal atom of different symmetry with respect to the MXM unit (e.g., $\sigma \rightarrow \pi$), one way it may proceed is via an electron "jump" when viewed on an orbital basis. Second, if the energies of the two (e.g., z^2) orbitals, one on each metal center, are very different so they do not cross in the style of Figure 8, the electron will need to jump from one to the other some time along the reaction coordinate. Also it is clear that if sudden electron transfer does occur, then there is no need for atom transfer to occur at all. Which metal center retains the bridging ligand will be determined by other factors.

One final point is that although in simple one-electron molecular orbital theory we envisage an electron jumping from one orbital to another, no energy is in fact absorbed or emitted at this point. The process is simply the intersection or avoided intersection of two potential surfaces in n-dimensional configuration space (Figure 11).

Application of These Results to Some Experimental Examples

The energy changes of Figure 6 represent the effect of moving the bridging group to an asymmetrical position in the binuclear complex. The diagram as a whole shows the energetics associated with atom transfer within this binuclear species. When viewing the kinetics of these redox reactions as a whole we must also allow for the fact that there may well be a barrier to formation of such a complex (asymmetric or symmetric) from six- and five-coordinate units. Thus the energy profile of the complete reaction may well be more complex than we have indicated in Figure 6. From the relative sizes of the barrier and well of Figure 6 steps involving precursor complex formation should be more noticeable for the type II pathway than for type I, due to the smaller energy changes in the latter system.

Our approach will neglect changes in solvation energy and electrostatic forces involved in bringing together the reacting ions. We shall focus on the energy changes involved in making the bridging atom of the symmetric structure asymmetric[39] as occurs in the atom-transfer process. As far as the metal d orbitals are concerned, this is equivalent energetically to forming a symmetrical structure from remote five- and six-coordinate structures. We shall ignore any relaxation of other ligands coordinated to the two metal centers since this is difficult to include using our simple molecular orbital method. In all cases we shall assume that the transition state or intermediate has a linear MXM geometry and use a classification scheme based on the type I and II processes.

$z^2 \rightarrow z^2$ **Transfer.** This is the simplest process of all and therefore the one we shall treat first. For the $Cr^{II}/Cr^{III}X$ system (hsd^4hsd^3, $\pi^6\sigma_g^1$) one electron is transferred from the z^2 orbital of Cr^{II} to the corresponding orbital on Cr^{III}. (This category of reaction has been previously referred to as "$e_g \rightarrow e_g$" transfer using octahedral labels.) This particular reaction was one of the first systems studied[40,41] with a view to defining the inner-sphere pathway with bridging ligands such as halide, N_3^-, SCN^-, NCS^-, OAc^-, etc. With H_2O, NH_3, and pyridine as bridging ligands the outer-sphere route is preferred.[42] In view of our previous discussion it is a typical example of passage over a type I barrier in which the electron transfer is a smooth one (Figure 7) and is induced by atom transfer. By use of our schematic notation it is described by **14** with

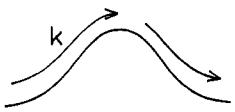

14

a rate constant k. In this case we do not have to worry about the electrons in the t_{2g} orbitals. There are always sufficient to singly fill all six π orbitals. The rate of the electron-transfer reaction is then determined by the height of the barrier at the symmetrical transition state. One series we shall find useful in our classification of the mechanism of these reactions is the dependence of rate on the nature of the halide bridge. For the $Cr^{II}/Cr^{III}X$ system the rates increase[40d,41a] in the order $X^- = F^- < Cl^- < Br^- < I^-$. This is called the "normal" order. The reverse order has been termed the "inverse" order. Simple molecular orbital calculations designed to reproduce this order are difficult to rely on. First we do not know the exact geometry (M–X bond lengths) for the symmetrical structure, and second we are at the mercy of the parameters of the method (orbital exponents and ionization potentials) when comparing the energetics of the fluoride bridge with an iodide bridge for example. However the results of the calculations do hint that whether the normal or inverse order applies may well be determined by whether the process is of type I or type II. For all electronic configurations giving rise to type I behavior the barrier to reaction decreased with increasing bridging halide size. This result was not very sensitive to the exact choice of geometrical and molecular orbital parameters. For type II behavior with a π^n configuration a similar insensitivity was found but the well depth increased with bridging halide size. For type II behavior with other electron configurations the results were dependent upon the parameters involved. Thus our cautionary conclusion is that the halide order may well be diagnostic of the reaction type, especially where the σ_g and σ_u orbitals are not symmetrically occupied—normal for type I, inverse for type II.

We have assumed in Figure 7 that the halves of the transition state are identical in that the energy levels are the same. This can be ensured by making the ligands coordinated to Cr^{II} and $Cr^{III}X$ the same. But what happens if the ligands are different? In order for a smooth transfer to occur the z^2 orbital initially on Cr^{II} must rise in energy and cross the z^2 orbital initially on the six-coordinate Cr^{III}. This would be the case in some asymmetric system, Figure 12a, but not in the case of Figure 12b. In the latter we would expect the system to initially move uphill and then experience an electron jump

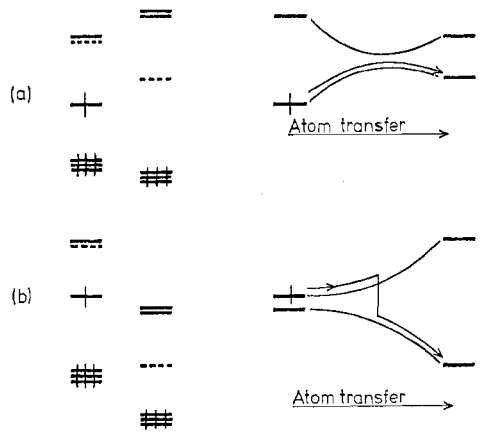

Figure 12. Two different mechanisms of electron transfer dependent upon the relative energies of donor and acceptor sites. In (a) the donor and acceptor orbitals cross on bridging atom transfer (cf. Figure 8) and the electron transfer is smooth. In (b) donor and acceptor sites do not cross and the electron transfer has to be of the sudden type, occurring somewhere along the reaction coordinate.

from the donor orbital to the acceptor orbital. If the electron jumps from one orbital to another as in Figure 12b, then there is no need for atom transfer to occur at all, as we have noted above. However the transferred electron ends up in a z^2 orbital which is metal–bridging ligand antibonding. On these grounds the bridging group will prefer to be bound to the metal atom which does not contain z^2 occupancy, i.e., Cr^{III}. So atom transfer occurs after all. One other way of viewing this effect is that Cr^{II} species are labile and Cr^{III} species inert. There is no well-documented case with this particular electronic configuration where bridging group transfer does not occur.

Cr^{II} is not the only reducing agent of this type with a single "e_g" electron. $Co(CN)_5^{3-}$ (low spin d^7) is another well-studied example.[43] Cr^{II} and $Co(CN)_5^{3-}$ reductions of Co^{III} systems (lsd^6) have also been extensively studied[44] and from the experimental point of view are very similar to $Cr^{II}/Cr^{III}X$ redox systems. We expect to observe simple type I behavior, but here however we have added complications. First, in the Co^{III} system there are six t_{2g} electrons which need to be accounted for during the atom-transfer process. We may simply get over this problem by putting the t_{2g} set of orbitals to lower energy on the Co^{III} than Cr^{II} (**15**). If they lay to higher energy than

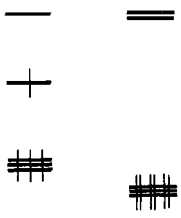

15

those of Cr^{II}, then flow of three electrons from Co to Cr would occur on complex formation. In practice this would not happen since the charge on the Co would be so drastically increased that the t_{2g} orbitals on this atom would drop to much lower energy. Flow of electrons back to the Co would occur. In many ways this complication arises from the fact that we are using a simple one-electron molecular orbital model with fixed atomic orbital ionization energies to view these complex processes. Our way of showing that the electrons do not flow toward the Cr on the simple MO approach is to place the t_{2g} orbitals to lower energy.

Second, the Co^{III} system is usually more stable as a low-spin $(t_{2g})^6$ system but the redox product Co^{II} is more stable as a high-spin $(t_{2g}^5e_g^2)$ system. A lot of effort has been devoted to this particular problem. Our molecular orbital approach allows us to answer this problem in a way different from all previous approaches by using the profile of **14** and realizing that if the spin change on reduction of Co^{III} occurs before the maximum in the energy profile, then it will affect the rate of electron transfer. If on the other hand it occurs after the maximum, then it will not affect the reaction rate. A large amount of research with inner-sphere processes and Co^{III} has involved reduction of the $Co^{III}(NH_3)_5X$ species. For $Co(NH_3)_6^{3+}$ by making use of published[45] Racah and $10Dq$ parameters we find that the low-spin form is favored over the high-spin form by about 17×10^3 cm^{-1}. For $Co(NH_3)_6^{2+}$ the high-spin form is favored over the low-spin form by about 8×10^3 cm^{-1}. If we assume that the maximum in the reaction profile occurs at an oxidation state of 2.5, then at this point by interpolation the system will prefer to exist as a low-spin complex. For this species therefore the rate constant will be independent of the spin change. For $Co^{III,II}(H_2O)_6$ however we find that the spin change occurs before the maximum in the energy curve and will therefore increase the reaction rate. Inner-sphere reductions of $Co^{III}(H_2O)_5X$ have been little studied due to their tremendous redox sensitivity which we suggest is due to this effect. We return to this point later in more detail when discussing outer-sphere reactions.

The relative reaction rates for halogen and other bridges are very similar in all systems irrespective of the nature of the metals in the oxidant or reductant, emphasizing a common intimate mechanism. For *cis*-$Co^{III}(en)_2XCl$ (X = NH_3, Cl, H_2O, py) reductions by Cr^{II} lead[46] to negative values of $\Delta H^{\ddagger}$. This is very good evidence for the formation of a precursor complex. As we have indicated above this must be geometrically of the form of the Pt^{II}/Pt^{IV} mixed-valence system, i.e., asymmetric. No intermediate has been detected in these reactions either spectroscopically or kinetically in agreement with the type I profile.

Completely analogous reactions to the ones we have discussed here occur between H atoms[47] and $Co(NH_3)_5X$ species. On a molecular orbital basis the H atom provides a σ orbital containing a single electron in an analogous way to the z^2 orbital on Cr^{II}. Atom transfer occurs, HX is produced, and the halide sensitivity order is $F^- < Cl^- < Br^- < I^-$, i.e., the normal order observed above for Cr^{II}/Co^{III} reductions. A similar mechanism to this reduction is expected for the two-electron transfer in the Pt^{II}/Pt^{IV} [48] system (lsd^8lsd^6, $\pi^{12}\sigma_g^2$). The situation is slightly different in that the square-planar Pt^{II} is doubly unsaturated and catalytic effects due to coordination of halide to the Pt^{II} site are to be expected and indeed observed. The halide sensitivity of the bridging ligand is again the normal one as seems typical for type I transfer processes.

Related in molecular orbital terms are the reactions of Co^{II} species with alkyl halides. Two possible modes of attack are possible with either the alkyl group[14] or halide playing the bridging role. Thus $Co^{II}(CN)_5^{3-}$ proceeds via a radical pathway[49a] (eq 2) where the halide acts as the bridge but

$$Co^{II}(CN)_5 + X\text{–}R \rightarrow [Co\text{–}X\text{–}R] \rightarrow Co^{III}(CN)_5X^{3-} + R\cdot$$
$$R\cdot + Co(CN)_5 \rightarrow RCo(CN)_5 \qquad (2)$$

$Co^{I}(DMH)_2PBu_3^-$ reacts[49b] via the direct nucleophilic pathway eq 3 by using the alkyl group as a bridge. Interestingly in eq

$$Co^{I}(DMH)_2PBu_3^- + R\text{–}X \rightarrow [Co\text{–}R\text{–}X] \rightarrow RCo(DMH)_2PBu_3 + X^- \qquad (3)$$

2 the rates increase[49a] in the order RI > RBr > RCl. Reactions proceeding via this radical pathway have also been observed for other X–Y systems,[49c] and this is a feature of some oxidative addition reactions.

$t_{2g} \rightarrow t_{2g}$ Transfer. We can divide these systems into two categories: one where there are electrons in the system in

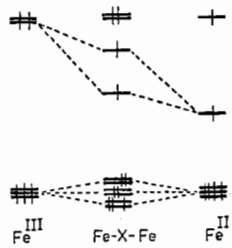

Figure 13. Molecular orbital pattern and electron occupancy of a binuclear complex formed from high-spin ferrous and ferric ions.

addition to t_{2g}-type electrons and one where the configurations of the two ions are t_{2g}^n and t_{2g}^m only. An interesting example of the former type is the $Fe^{II}/Fe^{III}X$ exchange (hsd^6hsd^5, $\pi^7\sigma_g^1\sigma_u^1$).[50] By way of contrast to the Co^{II}/Co^{III} system both oxidation states of hexaaquoiron prefer the high-spin configuration.[5] One interesting facet of the system is that the inner-sphere route is not all that faster than the outer-sphere one. The electron configurations of the two ions differ only in the presence of one t_{2g} electron, and the electronic configuration of the dimer is such that we predict a weakly bound symmetrical structure as an intermediate (Figure 13). An intermediate has in fact been detected kinetically for the case where $X^- = N_3^-$.[50b] Depending upon the temperature the rate of decay of the intermediate may be slower than the rate of its formation from five- and six-coordinate units. From our discussion above then, the electron transfer may occur in two parts. First, partial charge redistribution occurs during formation of the intermediate, and, second, the rest of the charge is transferred during decay of the symmetrical structure. This is of course assuming that the intermediate is a class IIIA mixed-valence species where both Fe sites are equivalent. If the intermediate is of class II with localized valences, then the majority of the charge transfer will occur on intermediate decay. Thus the scheme **2** needs to be modified by removal of the "electron-transfer" step. Electron exchange occurs during formation and/or decay of the intermediate. Since the intermediate is predicted to be rather loosely held together, we should not be too surprised that the electron-transfer rates in these systems are similar to those via the outer-sphere route. The experimentally observed halide sensitivity[50,51] in this series of reactions is in the inverse order, in contrast to the redox systems of the previous section. Although our molecular orbital calculations are not clear on this point for this particular electronic configuration, this inverse order may be general for all type II processes.

Many systems containing t_{2g} electrons only are known as crystal structures as we have seen above. Others have been observed in redox solutions by spectroscopic methods (Table I). For example reactions of V^{II} and $V^{IV}O$ systems (hsd^3d^1, π^4) lead to ready detection of VOV^{4+}, and similar species[52] are observed with Cr in agreement with our prediction. Redox behavior here occurs in an exactly analogous way to the $Fe^{II}/Fe^{III}X$ system above. As we have noted above, it is probably meaningless to try to follow the electron-transfer process on an orbital basis in these π^n systems but one example where it is difficult to envisage any process other than an electron jump is the reduction of Cr^{VI} or V^V by ferrocyanide[53] (d^0lsd^6) (Figure 14). Under these electron jump circumstances bridging group transfer is not necessary for electron transfer and indeed in this particular system the bridging CN^- ligand is retained by the Fe. What decides which metal the bridging ligand remains attached to depends upon the relative bond strengths to each metal. CN^- will surely prefer the softer Fe^{III} to the harder Cr^V or V^{IV}.[54] In some cases it is possible to observe kinetically the rate of formation and decay of the bridged species. For example in the V^{II} or Eu^{II} reduction of VO^{2+} systems, both steps may be observed.[52b,55]

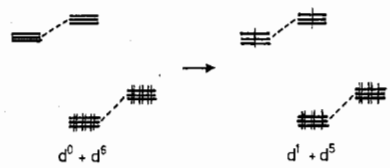

Figure 14. Schematic electron-transfer process for the oxidation of ferricyanide by Cr^{VI} or V^V.

$z^2 \rightarrow t_{2g}$ Transfer. This is overall a symmetry-forbidden process, although by bending the MXM unit we could remove the distinction between σ- and π-type interactions. Intermediates have been detected for reactions of this type giving us vital clues as to their intimate mechanism. For example with Cr^{II} reductions of a range of chlorine-containing Ru^{III} systems there is a ready detection of $Cr^{III}ClRu^{II}$ intermediates[56] where the oxidation state assignments are from spectroscopic data. Similar complexes with adjusted oxidation states compared to reactants are found for Cr^{2+} and VO^{2+} (Cr^{III}, V^{III} hsd^3hsd^2), $Co(CN)_5^{3-}$ and $IrCl_6^{2-}$ (Co^{III}, Ir^{III} lsd^6lsd^6),[58] and $Co(CN)_5^{3-}$ and $Fe(CN)_6^{3-}$ (Co^{III}, Fe^{II} lsd^6lsd^6)[59] among others. A binuclear intermediate is claimed for reduction of V^{III} by Cr^{II} from kinetic evidence.[60] In each case production of a stable intermediate is in accord with our molecular orbital ideas above. The electronic configuration of all the examples is π^n. In some systems, e.g., Cr^{II} reduction of Ru^{III}(carbox) complexes, both the rate of formation and decay of the intermediate may be simply measured.[56c] Bearing in mind our discussion above we may view the overall process as in **16**.

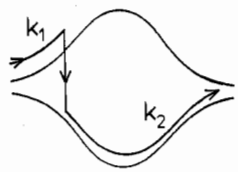

16

The system moves partly along a type I profile, typical of the presence of a single z^2 electron in the system (hsd^4lsd^5), followed by sudden electron transfer from the z^2 orbital to a t_{2g} orbital (hsd^3lsd^6). Now the profile is of type II, and the intermediate with adjusted oxidation states is stable. Finally the intermediate decays. We remind the reader at this stage that no energy is absorbed or released during the sudden electron-transfer process. In **16** the two curves are separated for illustrative purposes only. As with the Cr^{VI}/Fe^{II} example above there is no restriction on how the bridged species may decay. It is not a vital part of the electron-transfer process. In fact for the $Ru^{II}ClCr^{III}$ bridged species, decay to both Cr^{III} and $Cr^{III}Cl$ in acid media is observed[56a] with more preference for Cr–Cl fission in neutral solutions (suggesting a contribution from a Ru^{II}–Cl–$Cr^{III}OH^{3+}$ intermediate).

Some observations which have a vital bearing on this reaction scheme are from the Cr^{II} reductions[56c] of Co^{III}(carbox)$(NH_3)_5$ and Ru^{III}(carbox)$(NH_3)_5$. As we have noted above, the Co^{III} system is described by type I whose rate is determined by passage over a barrier which in **16** the Ru system only climbs a part. One of the key points of the carboxylic acid series is that subtle variations in rate may be made by varying the bridge substituents. In Table II we see that the relative rates of reaction of the Cr^{II}/Co^{III} system are very similar to the relative sizes of k_1 for the Cr^{II}/Ru^{III} system. Indeed they should be on our scheme since both systems climb a type I barrier. Another feature of interest is that although the driving forces for the two reductions are similar (as measured[61] by the $Cr^{II,III}/M^{III,II}$ couples) the Ru k_1's are much faster than in the Co case. Again this is to be expected if the Ru system only climbs a part of the type I profile but the Co system climbs to the top.

Table II. Some Rates of Reactions between Cr^{II} and (carbox)$M^{III}(NH_3)_5$ [M = Co, Ru (from ref 56c)]

(a) Relative Rates of Reactions[a]

carbox	M = Co	M = Ru
O_2C-H	55	43
O_2C-CH_3	2.1	6.5
O_2C-$C_6H_4CH_3$	1.3	1.7
O_2C-C_6H_5	1.2	1.5
O_2C-p-C_6H_4OH	1.0	1.0
O_2C-CF_3	0.8	0.4

(b) k_1 and k_2 for Cr^{II} + (carbox)$Ru^{III}(NH_3)_5$

carbox	k_1, M^{-1} s^{-1}	k_2, s^{-1} (at 25 °C)
O_2C-H	1.7×10^5	2.4
O_2C-CH_3	2.6×10^4	25.5
O_2C-$C_6H_4CH_3$	6.6×10^3	*b*
O_2C-C_6H_5	5.8×10^3	*b*
O_2C-p-C_6H_5OH	4.0×10^3	>29[c]
O_2C-CF_3	1.4×10^3	*b*

[a] For M = Co this is k; for M = Ru this is k_1. [b] Too fast to measure at 25 °C. [c] Rate was 29 s^{-1} at 10 °C.

One further feature of the Ru^{III}(carbox)$(NH_3)_5$ system we shall analyze in a little more detail is that in general fast k_1's correspond to slow k_2's and vice versa.[62] In **17** we see the

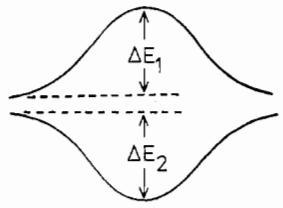

17

activation energy contributions from the σ orbital containing the unpaired electron initially on the Cr^{II} z^2 (ΔE_1) and from the π-orbital manifold (ΔE_2). The rate constant k_1 will be determined by $\Delta E_1 - \Delta E_2$ and k_2 by ΔE_2 alone. We have analyzed the effect of variation of bridge substituent by performing extended Hückel calculations on a model carboxylate-bridged system. For the series of substituents of Table II our results show that the energy of the lowest σ-type orbital in the symmetric transition state (which determines ΔE_1) is insensitive to the nature of the substituent R (**18**).

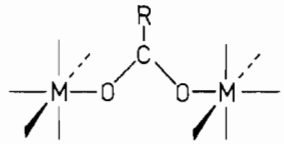

18

This perhaps surprising result arises because the lowest energy σ orbital is the antisymmetric one and is largely located on the metal and oxygen atoms (**19**). By way of contrast ΔE_2

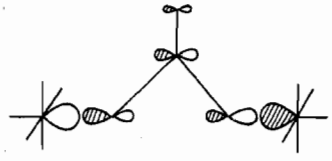

19

is sensitive to variation in the nature of the substituent R by virtue of the fact that one of the π set of orbitals contains significant contributions from R (**20**). This particular orbital is destabilized as the p-orbital contribution from the α carbon atom increases, as it does in the order R = H (no contribution) < R = CH_3 < R = Ph. Thus ΔE_2 increases in the order Ph

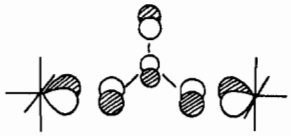

20

< CH_3 < H, and k_1 is predicted to increase in the order Ph < CH_3 < H (order of decreasing $\Delta E_1 - \Delta E_2$) and k_2 to increase in the reverse order H < CH_3 < Ph. This is just the experimental order.[56c] Furthermore for the Co^{III} reduction the change in $\Delta H^{\ddagger}$ for the reaction is experimentally about 0.7 kcal mol^{-1} on going from R = H to R = Ph. We calculate a figure of 1.1 kcal mol^{-1} for our model system with two Cr atoms. This imaging behavior of k_1 and k_2 supports our ideas depicted in **16** rather well.

More information is contained in results on the reduction of $Ru^{III}(NH_3)_5X$ and $Co^{III}(NH_3)_5X$ (X = halide) systems.[56c] For the Co^{III} system the rate dependence on halide is the normal order I > Br > Cl (ratio 5:2:1) but in the Ru^{III} system the order is reversed (ratio $1:10:10^2$). In the latter case the reaction is characterized by a fast reaction to form intermediate followed by relatively slow rate-determining decay. So the rate-determining step in the cobalt case is k of **14** and in the ruthenium case is k_2 of **16**. In each case the halide sensitivity is in the direction we have now come to associate with type I (normal order) and type II (inverse order) behavior.

For the related Eu^{2+} (d^0f^7) reduction of Ru^{III} we also see the inverse order Cl > Br (2:1) for the rates[63] of decay of the intermediate.[64] Here the reducing electron comes from the structurally impotent f-orbital manifold. In this case the rates of formation and decay of the intermediate could be measured. (The Eu^{II} and Cr^{II} reductions share the k_2 path.)

A process related to the $z^2 \rightarrow t_{2g}$ transfer above is the Cr^{II} reduction[65] of $U^{VI}O_2^{2+}$ and its Np analogue (hsd^4d^0). Here the z^2 electron on Cr^{II} is transferred rapidly to the actinide center and the predicted binuclear intermediate (hsd^3d^0, π^3) readily observed is of the type $(H_2O)_5Cr^{III}$–O–U^{V}–O^{4+}.

A different surface pertains to the $Cr^{II}/Fe^{III}X$ system[66] where the $Fe^{III}X$ species is present as a high-spin complex. Here initially there are two electrons in z^2 orbitals leading to type II behavior. After the electron jump $z^2 \rightarrow t_{2g}$ the presence of one z^2 electron demands type I behavior (**21**). The electron

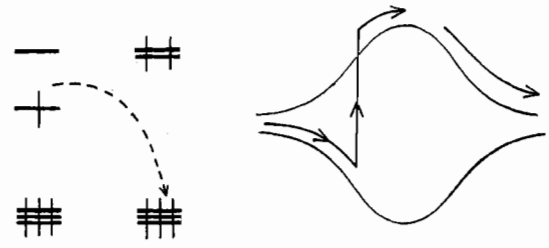

21

jump may occur before or after the symmetric structure. Since the halogen sensitivity is in the normal order, then perhaps the situation is as shown in **21**. No intermediate has been detected experimentally in this system.

$t_{2g} \rightarrow z^2$ Transfer. This is the overall process occurring in inner-sphere reductions of, e.g., Co^{III} by V^{II} and we may envisage this to occur in the opposite direction to **14** above (**22**).

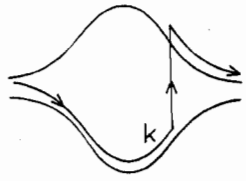

22

Analogous reactions occur with the d^0 systems Eu^{II} (f^7)[67] and U^{III} (f^3)[68a] where the reducing electron comes from the f-orbital manifold. We will discuss these examples since the V^{II} reductions often proceed via the outer sphere route, due to the inert nature of this d^3 configuration. The rate dependence on bridging halide is the inverse one in both systems suggesting the behavior in **22** rather than the behavior in **23**. In many

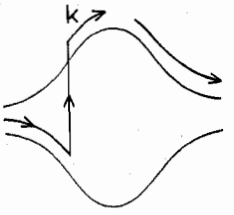

23

of these systems a large excess of reductant was used precluding the ready observation of an intermediate but one has been observed kinetically[68a] for $U^{III}/Co^{III}(NH_3)_5H_2O$ where an OH bridge is present. In the U^{III} reduction of $Cr^{III}X$ systems the halide sensitivity is the normal one and a binuclear intermediate is indicated on kinetic grounds.[68b]

This t_{2g} to z^2 process also occurs with the Fe^{II} reduction of Co^{III} (hsd^6lsd^6).[63,69] Since the Fe^{II} is high spin and contains a z^2 electron, the reaction profile (**24**) is laterally inverted from

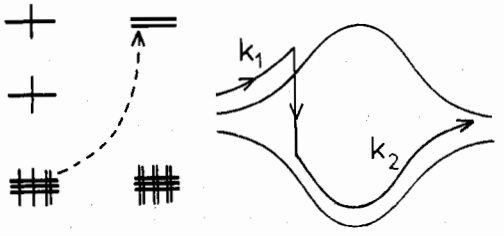

24

16. Here after the electron jump there are two z^2 electrons present and the type II profile applies. For Fe^{II} reduction of $Co^{III}(NTA)(NH_3)_5$ (NTA = nitrilotriacetic acid, $N(CH_3CO_2)_3^{3-}$) an intermediate has been detected[70] but this apparently with oxidation states Fe^{II} and Co^{III}. No intermediate has been detected in the halide case.

$x^2 - y^2 \rightarrow z^2$ or t_{2g} Transfer. This reduction process occurs[71] in reactions of Cu^I with $Co(NH_3)_5X$ ($d^{10}lsd^6$). The overall electron transfer results in the system moving from a $\pi^{12}\sigma_g^2$ configuration to a $\pi^{12}\sigma_g^2\sigma_u^1$ configuration (**25**) both of which

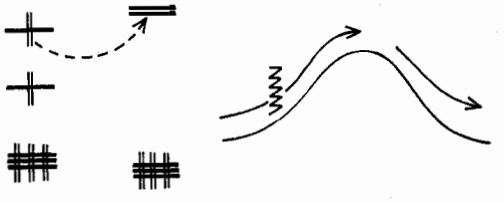

25

demand type I behavior. No intermediates have been experimentally observed. The halide sensitivity is in the normal order in agreement with this profile.

Similar behavior is expected for Cu^1 reductions of t_{2g}^n ($n < 6$) systems. Here the electronic configuration changes from $\pi^n\sigma_g^2$ to $\pi^{n+1}\sigma_g^2$, and type I behavior with no detectable intermediate is expected. Indeed Cu^I readily reduces[72] VO^{2+}, and out of all four reductants studied to date[52,55,72] (V^{II}, Cr^{II}, Eu^{II}, Cu^I), the Cu^I reduction was the only one where an intermediate was not observed, in agreement with our ideas.

Other Systems. One system which does not readily fit into our classification above is the Eu^{II} reduction[66] of $Fe^{III}X$ systems (d^0hsd^5). We recall that the Eu^{II} reduction of t_{2g}^n systems led via a type II profile to a detectable intermediate. However

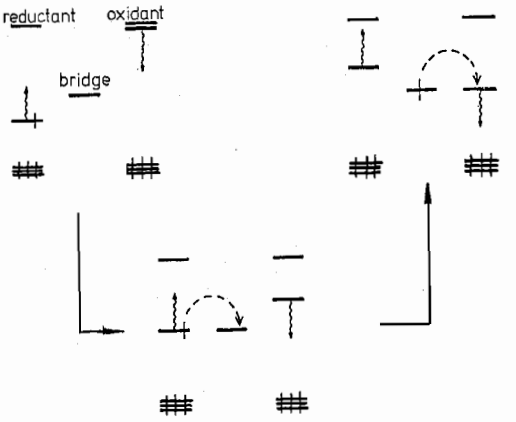

Figure 15. Schematic electron-transfer process between Cr^{II} and Cr^{III} when the bridging ligand has a low-lying orbital.

the single z^2 electron on the high-spin Fe^{III} means that things will be a little different. Since this electron remains with the Fe unit and is not involved in the transfer process, then the relative arrangement of orbitals on reductant and oxidant will be like that of Figure 12b with occupation of the lower energy, oxidant z^2 orbital. This orbital decreases in energy until the sixth ligand is lost leading to a completely downhill path for ligand loss, **26**. In fact which metal ion retains the bridging

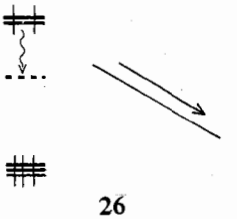

26

ligand will depend on the relative substituent lability of Eu^{III} and Fe^{II} centers. There is good experimental evidence[66] that after sudden electron transfer the Fe^{II} retains the bridging atom. The halide sensitivity is in the inverse order but it is difficult to tie this to our previous molecular orbital ideas.

Reducible Ligands. The chemical mechanism of electron transfer where the bridge group is chemically reduced (eq 1) and the M^{II}/M^{III} redox process occurs via a bridged $M^{III}X^-M^{III}$ species was excluded for most inorganic ligands.[10] However with some organic ligands as bridges there is the possibility of a low-lying bridge level which can allow facile transfer from M^{II} to ligand somewhere along the reaction coordinate. This is shown schematically in Figure 15 where as the energy of the z^2 orbital on Cr^{II} rises it may climb above the empty bridge ligand level. Later along the reaction coordinate the electron is finally transferred to the other metal atom. For the Cr^{II}/Cr^{III} system (hsd^4hsd^3) this transfer leads us to a hsd^3hsd^3 system which should be stable as a symmetrically bridged intermediate (π^6). The energy profile of the electron-transfer process is shown in **27**. Obviously this

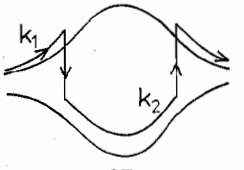

27

is a way of increasing the reaction rate since the full type I activation energy is not felt. Thus the glyoxylate complex **28**

$$\left[(NH_3)_5Co\text{-}O\text{-}\overset{\overset{O}{\|}}{C}\text{-}CHO\right]^{+2}$$

28

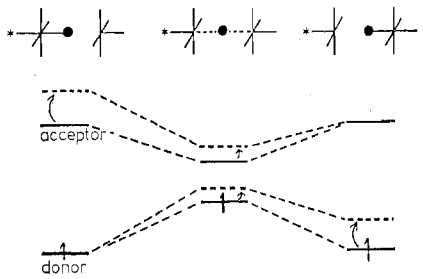

Figure 16. Energy modification of the σ orbitals (dashed energy levels) in the M_2X_{11} unit by the presence of a stronger σ donor trans to the bridging atom in the acceptor (labeled with an asterisk). The barrier for electron transfer (atom transfer) is increased.

is reduced $\sim 2 \times 10^3$ times faster[73] than the glycolate complex **29** by utilization of the chemical mechanism. If the electron

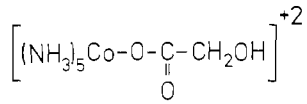

29

jump occurs early in the reaction coordinate, then the reaction rate will not be very sensitive to the nature of the oxidant (e.g., Cr^{III} or Co^{III}) and this seems to be the case.[73,74] The rates of reduction by Cr^{II} of these two systems are very different with halide bridges but very similar with reducible ones. Such a leveling phenomenon will only be true for oxidants which receive a z^2 electron. For the reduction of the Ru^{III} analogue the rate is several orders of magnitude faster than in the Cr^{III} or Co^{III} cases. Here the reaction proceeds via a different route (vide supra) by a sudden electron jump to the π manifold. An intermediate has been observed in some cases. For example on mixing Cr^{II} and $Co^{III}(NH_3)_5L$ (**30**) an intense coloration

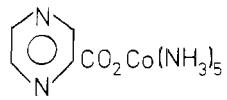

30

develops[75a] which is suggested to be the intermediate Cr^{III}–L^-–$Co^{III}(NH_3)_5^{4+}$ which we predicted might be observed in **27**. The ESR spectrum of this reduced intermediate has recently been observed.[75c] For reduction of the same species by Cu^+ there is no experimental evidence[75b] for formation of an intermediate under analogous conditions. This is quite understandable. After an electron has been transferred to the bridging ligand, the metal electronic configuration is still $\pi^{12}\sigma_g^2$ (the transferred electron came from $x^2 - y^2$) which demands a type I profile throughout, in contrast to the change to the type II profile in the Cr^{II} system (**27**) after the jump. Molecular orbital calculations designed to predict which systems will proceed via the chemical mechanism have been performed.[76]

Effect of Nonbridging Ligands. This is an area where molecular orbital theory was well in advance of detailed experimental studies.[77] Orgel[12] argued that the energy of the z^2 acceptor orbital would be very important in determining the rate of reaction since how stable or unstable this level was determined how easily the reducing electron could be transferred into it. Since the z^2 orbital was mainly involved in bridging and trans ligand interactions, the rate of reaction should then be sensitive to the nature of the trans ligand on the oxidant in addition to being very much affected by the nature of the bridge. Orgel argued that large Dq ligands in the trans position would slow down the reaction by pushing up this z^2 acceptor level. However, it has been pointed out[78] that is is σ strength that counts in this argument rather than $10Dq$ which is affected by σ and π effects. Also the nature of the cis ligands is not completely immaterial. On overlap grounds[79] the energy of z^2 is determined 4 times as much by trans ligand variations compared to cis ligand variations. In order to understand the observed trans ligand sensitivity we need to use a σ-strength order derived from an analysis of the electronic spectra of $Cr^{III}L_5Z$ systems (L = NH_3, H_2O) where the difference between two electronic transitions (**31**) tells us

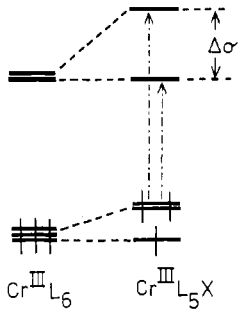

31

about the relative effectiveness in z^2 elevation by the ligand Z. Two studies are available which are unfortunately somewhat contradictory. Perumareddi[80] gives, for increasing $\Delta\sigma$, $I^- < Br^- < Cl^- < F^- < N_3 < H_2O < NCS^- < CN^-$, and Schäffer[81] gives $Br^- < Cl^- <$ py $< NH_3 < F^-$ ($< H_2O$), although H_2O is not well located in this order. Experimentally[82] the reaction rates of Cr^{II} reductions of $Co^{III}L_4XT$ vary with the nature of the trans ligand T in the order $Cl^- > H_2O >$ py $> NH_3 >$ en and $Cl^- > NCS$ which is in good overall agreement with the spectroscopic σ-donor order, although the position of H_2O is somewhat variable in the experimental series. A correlation has been published between log (rate) against energy of the highest energy dd electronic transition on the oxidant.[83]

We may view the effect of the trans ligand on the reaction rate very simply by modification of Figure 7 (Figure 16) where we show the effect of increasing the σ strength of a trans ligand on the oxidant. (The transition state feels a reduced effect of the trans ligand.) A higher barrier for Cr^{II} reduction of Cr^{III} or Co^{III} results.

These redox reactions are often catalyzed by halide ion. This is usually regarded as a thermodynamic effect, but we may see what happens to the barrier for the system where a halide ion has been removed from solution and coordinated in the reductant (eq 4). The effect is in the opposite direction

$$Cr^{II}(H_2O)_5 + Hal \rightarrow Cr^{II}(H_2O)_4Hal$$
$$Cr^{II}(H_2O)_4Hal + Co^{III}(NH_3)_5X \rightarrow (H_2O)_4HalCr\text{–}XCo(NH_3)_5 \rightarrow \text{etc.} \quad (4)$$

to that described for the acceptor trans ligand. Figure 17 shows the effect of increasing the σ strength of a ligand coordinated to the donor. Thus strong σ-donor ligands on the donor metal should accelerate the reaction. This is experimentally found to be the case; F^- is much more effective[84] than Cl^- ($F^- >> Cl^- > Br^-$).

For the Fe^{II}/Co^{III} redox system similar effects[85] are seen; in general the effects are more pronounced than for the Cr^{II}/Co^{III} system. The effects of coordinated ligands are readily understood for the k_1 path of **24** since the situation is identical with that in the Cr^{II}/Co^{III} system, but for the k_2 path arguments need to be based on the relative raising and lowering of various energy levels of Figures 16 and 17 and are unfortunately not amenable to qualitative analysis.

Extension to Outer-Sphere Reactions. The outer-sphere transition state has not received very much experimental study. However, there are indications that some sort of relative alignment between the two molecules is necessary.[86] For oppositely charged ions the outer-sphere "complex" resembles an ion pair.[87] For reactions between ions of like charge the

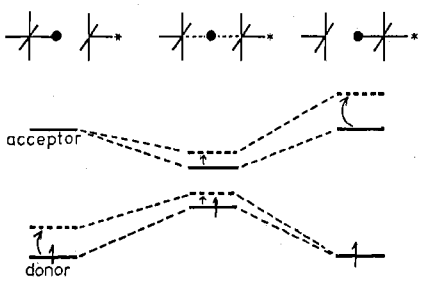

Figure 17. Energy modification of the σ orbitals (dashed energy levels) in the M_2X_{11} unit by the presence of a stronger σ donor trans to the bridging atom in the donor (labeled with an asterisk). The barrier for electron transfer (atom transfer) is decreased.

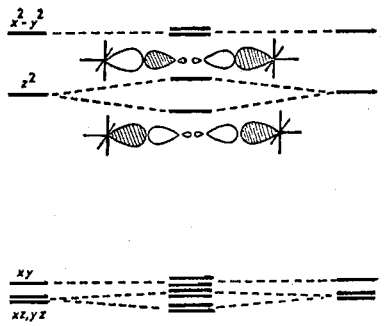

Figure 18. Schematic molecular orbital picture (not to scale) for the M_2X_{12} unit.

electron-transfer process is usually strongly counterion catalyzed; i.e., a negatively charged ion may hold together two positively charged units (just as the electron holds together the nuclei in H_2^+). Let us assume for the sake of simplicity that alignment of the C_4 axes of the reacting ions occurs. This leads to a geometrical arrangement strongly reminiscent of the inner-sphere situation except with two atoms or groups in the bridging position. On redoxidation the (e.g.) Cr^{II} system contracts and the (e.g.) Co^{III} system expands its coordination sphere as we have seen above. Thus the concerted motion is very similar to that in the inner-sphere case (**32**) where we use a diatomic (e.g., CN^-) ligand to reinforce the analogy.

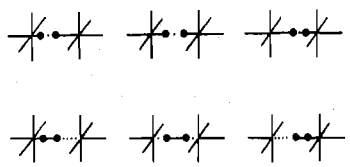

32

In view of the similarity of the two mechanisms how many of the inner-sphere considerations carry over into the outer-sphere process? The answer is virtually everything with some qualifications due to differences in the nature of the bridging groups. The form of the molecular orbital diagram is identical with that of the inner-sphere complex (Figure 3) for the symmetrically bridged structure. The exact description of the molecular orbitals is however different (Figure 18). As before, the σ_g^1, σ_g^2, and $\sigma_g^2\sigma_u^1$ configurations are predicted to be unstable in the symmetric arrangement, and all others should lead to stable symmetric structures. An exactly analogous diagram to Figure 7 applies to the description of the asymmetrization process. In general the splittings between the in- and out-of-phase components in Figure 18 will be less than those found in the comparable inner-sphere case, simply because the bulk of the electron density is metal located and poor overlap occurs between the molecular orbitals of the six-coordinate units. We can therefore, envisage type I and type II behavior in a way exactly analogous to that given before. The energy separation between σ_u and σ_g orbitals is a useful parameter in deciding on how large the type I barrier will be. Perturbation theory arguments suggest that the larger this splitting, the smaller the barrier to electron transfer. Obviously the larger the overlap between the two bridging ligands, the larger is the splitting and the smaller the barrier. This is fairly obvious—the larger the interaction between the two molecules, the easier it should be to "transfer" the electron. Experimentally the outer-sphere halide sensitivity is always the normal one. This may be due to the larger overlap of the terminal I ligand with another molecule.

It is interesting to ask at this stage how we may, for a given system, increase the σ_g/σ_u splitting such that the barrier to type I electron transfer is reduced. One way of doing this is to introduce another species into the space between the reacting ions, **33**. σ_g and σ_u will be shifted in energy and the overall

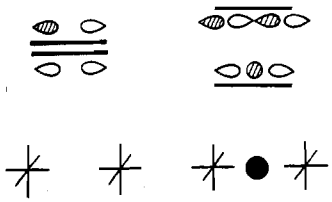

33

effect will be an increase in the energy between them. Increased coupling between the metal centers is found, and a much reduced barrier to electron transfer results. Our calculations on model systems show that the barrier may be dropped by 1–2 kcal mol^{-1} for insertion of a Na^+ ion between lsd^6 and lsd^7 ions separated by ~9 Å. Catalysis of outer-sphere reactions by added counterions certainly occurs,[88] although this has not been a well-studied field. The general conclusions are that the effects of anion or cation catalysis are not simply due to reduction of electrostatic interactions. Our molecular orbital ideas here provide an additional mechanism for its operation. The effects are sometimes very drastic. In reductions[88b] of $Co(NH_3)_6^{3+}$ and $[(NH_3)_5Co]_2NH_2^{5+}$ by V^{II} the ratios of k_{cat}/k_{uncat} are about 10, 10^3, and 10^5 for the ions Cl^-, SO_4^{2-}, and F^-.

The molecular orbital effect operating here is exactly analogous to the splittings noted in Figure 3 when the bridging ligand was inserted between the two five-coordinate units of the inner-sphere complex. As we noted above, this has been called[17] through-bond coupling. The barrier to electron transfer is reduced and in addition the resonance energy ($\Delta\epsilon/2$ of Figure 2) is increased as an added bonus. Our model calculations on this system indicate that $\Delta\epsilon$ is increased from ~0.07 kcal mol^{-1} (for the system without Na^+) and probably then described by nonadiabatic behavior to about 1.5 kcal mol^{-1} (with Na^+ present) and described by adiabatic behavior. Thus the effect of the counterion may be threefold: (i) acting as an electrostatic glue, (ii) reducing the barrier to reaction, (iii) ensuring adiabatic behavior. Although we have concentrated on the type I barrier, similar arguments apply to type II behavior. The overall result is that the depth of the well is decreased when the extra species is inserted between the two ions. Indeed, the $Fe(CN)_6^{3-}$–$Fe(CN)_6^{2-}$ exchange is strongly catalyzed by counterions. For our model system the well depth decreases by about 0.5 kcal mol^{-1} on insertion of the Na^+ ion with this (lsd^6lsd^5) electron configuration.

In addition to charged counterions which may be inserted between the two reacting ions what other likely catalysts are there? The requirement for a good catalyst is that it be able to stabilize differentially either the σ_g or σ_u component of the bridge orbitals. One system which could stabilize the σ_u component and leave the σ_g orbital virtually untouched is that of ethylene-type molecules where we have an accessible π

orbital, **34**, and no accessible symmetrical orbitals. In the same

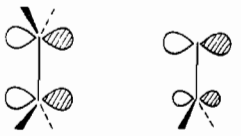

34 **35**

class would be ketone molecules, **35**. But probably the most important catalyst of all according to these arguments would be the water molecule itself, i.e., the very solvent in which all these reactions are performed! It possesses an antisymmetric b_2-type orbital (as HOMO) which (**36**) is ideally located to

36

perform this task. The orientation of the molecule with respect to the terminal metal-bound ligands would probably be along the lone-pair directions. Our model calculations with an H_2O located between the reacting ions show a drop in energy of activation of $\sim$4 kcal mol^{-1} and an increase in resonance energy of $\sim$6 kcal mol^{-1}. Thus it does appear that the solvent plays quite a vital role in these outer-sphere redox processes.[89] It would be interesting in the light of this result to carry out more extensive studies of redox systems in other solvents.

In contrast to the type I and II transfer processes we have focused on above where no electron jump occurs, when sudden transfer occurs the rearrangement energy expended can be regarded as the energy necessary to achieve the "common state" required for the Franck–Condon transition. In general some electron transfer will have occurred before this position is reached, so the sudden electron transfer may not involve a "full" electron. These arguments are of course exactly analogous to the earlier discussion on inner-sphere energetics. On this basis then outer-sphere reactions occur in a very similar way to the inner-sphere ones on a molecular orbital basis. "$e_g \rightarrow e_g$" transfers are slow because a sizable barrier needs to be surmounted; "$t_{2g} \rightarrow t_{2g}$" reactions are much faster since now the symmetric geometry corresponds to a stable structure and there is a potential well in contrast to a potential barrier here. These ideas dovetail nicely with previous arguments concerning the relative rates of these reactions; i.e., the rearrangement energy is small for $t_{2g} \rightarrow t_{2g}$ but large for $e_g \rightarrow e_g$ reactions. The phenomenological Marcus theory carries over well into the intimate mechanism described here.

The only really serious failure of the Marcus treatment, however, applies to reactions involving the hexaaquocobalt species. The reason for this[90] has been pinpointed as due to the spin change inherent in going from Co^{III} $(t_{2g})^6$ to Co^{II} $(t_{2g}^5e_g^2)$. Reactions of $Co^{III}(H_2O)_6^{3+}$ occur much faster than theory predicts while reductions of $Co^{III}(NH_3)_6^{3+}$, a closely related system, are well fitted by theory. We may very simply extend the inner-sphere discussion on this problem to the outer-sphere case. For outer-sphere reduction of Co^{III} species by Cr^{II} there will be two energy surfaces representing Cr^{II} oxidation by low- and high-spin Co^{III}. The low-spin curve is a simple type I process as we have discussed at length earlier. The high-spin curve is of mixed type since here the overall redox process is a $z^2 \rightarrow t_{2g}$ transfer and will be similar to the Cr^{II} reduction of Fe^{III} described earlier. Whatever the exact details of the shape of this curve three possibilities occur (Figure 19), equally applicable to both inner- and outer-sphere reactions. The low-spin and high-spin curves may cross after the maximum in the lower curve (Figure 19a) in which case the rate is unaffected by the spin change and the Marcus predictions hold. This is the situation with $Co(NH_3)_6^{2+,3+}$ where we discussed the problem for the inner-sphere case

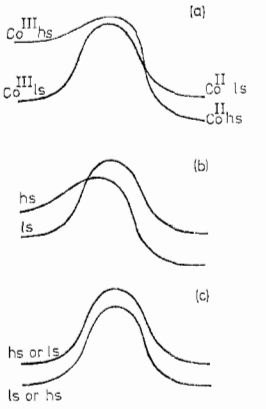

Figure 19. Influence of the spin change on Co^{III} on reduction of the barrier height to electron transfer (ls, hs = low spin, high spin): (a) spin change occurs after the maximum in the low-spin curve and does not affect the rate; (b) spin change occurs before the maximum and the rate is increased; (c) no spin change occurs at all.

earlier. Alternatively, if the curves cross before the maximum, then the spin change will affect (Figure 19b) the reaction rate. It will be greatly accelerated since the full activation energy of the lower curve is not felt. This is the case with H_2O as a ligand. The third case (Figure 19c) is where the two curves do not cross at all. An example here is the $Co(terpy)_3^{2+,3+}$ system[91] where the low-spin configuration is stable throughout. Thus, although we do observe a spin change in for example $Co(bpy)_3^{2+,3+}$ species (Figure 19a), the reaction rate is very similar[90] to that for the $Co(terpy)_3^{2+,3+}$ reaction (Figure 19c). Only for the situation in Figure 19b should any effects of the spin change be seen[92] on the reaction rate.

Considerations similar to the ones we used before to look at the effect of nonbridging ligands in the inner-sphere case apply here as well. The potential barrier of Figure 18 may be increased or decreased according to the nature of the ligands coordinated to the oxidant and reductant. For example in reductions of Co^{III} complexes, $Co^{III}(NH_3)_5(H_2O)$ is reduced faster[88c] than $Co^{III}(NH_3)_6$, and $Co^{III}(en)_3$, less rapidly than $Co^{III}(NH_3)_6$ in agreement with the σ-donor order we discussed previously.

Of course our discussion here does not supersede the Marcus treatment in the least. Ours is not a quantitative approach to reaction rate constants at all, but a theoretical description of the intimate mechanism of the redox process. As we have just seen, it may give clues as to when the phenomenological treatment could break down.

Discussion and Conclusion

At this stage it is interesting to see how our results fit into an overall view of electron-transfer processes. Let us look at the mode of transport in the symmetrically bridged intermediate—the intimate details of this process we have rather glossed over—which impinges directly into the field of mixed-valence chemistry. In simple orbital terms we may view the transport process, the electron hopping back and forth from one site to another, by using the diagram of Figure 8. Here we saw that the donor and acceptor levels (z^2 orbitals in this case) moved up and down in response to the movement of the bridging atom. Along similar lines for the mixed-valence species the "reaction coordinate" may be bond deformations or stretching of bonds not directed toward the other half of the molecule. In addition the orbital energies will depend upon the charge on each metal atom, and this will change as the electron is "transferred" from one atom to the other. A similar process is envisaged[93] for carrier transport through van der Waals solids, where the term softaron has been coined[94] to describe the motion of a trapped electron or hole (cf. polaron) from one site to another via a soft geometrical distortion.

Table III

orbital	H_{ii}, eV	exponent	orbital	H_{ii}, eV	exponent
Cr 4s	−9.00	1.700	Na 3s	−5.10	0.733
4p	−5.00	1.700	3p	−3.00	0.733
3d	−11.50	4.95 (0.4876), 1.60 (0.7205)[a]	C 2s	−21.40	1.625
			2p	−11.40	1.625
F 2s	−40.00	2.425	N 2s	−26.00	1.950
2p	−18.10	2.415	2p	−13.40	1.950
Cl 3s	−30.00	2.033	O 2s	−32.30	2.275
3p	−15.00	2.033	2p	−14.80	2.275
I 5s	−20.00	2.00	H 1s	−13.60	1.300
5p	−12.00	2.00			

[a] A double-ζ set was used for the Cr 3d orbitals. The mixing coefficients of the two parts are given in parentheses.

Whereas the energy changes on atom transfer were readily visualized for the σ levels (Figure 7), the weighing of the energy changes involved in the π manifold associated with this and other types of deformations is much less accessible using a simple molecular orbital approach.

So we have been successful in this paper in rationalizing the overall kinetic behavior for several of these redox systems, but only in certain cases and in certain parts of mechanisms have we been able to specifically indicate in orbital terms how the electron-transfer has occurred. The electronic charge distribution in symmetrically bridged systems and how this changes on decay of such a structure are at present beyond our simple approach.

Acknowledgment. This work was performed during the author's leave of absence at Cornell University and was supported by the National Science Foundation through Grant CHE-7606099. I wish to thank Professor Roald Hoffmann for his splendid hospitality and generosity during this period and also other members of the Cornell group for useful discussions and conversations concerning this work. My thanks also go to E. Kronman and R. Albright for typing the manuscript.

Appendix

Calculations of the extended Hückel type[35] were performed on some model systems with the exponents and diagonal matrix elements (H_{ii}) given in Table III. Off-diagonal matrix elements were approximated using the arithmetic mean Wolfsberg–Helmholtz formula with $K = 1.75$.

The inner-sphere $Cr_2Cl_6X^{6-}$ system was the model complex used to analyze the effects of variations in the bridging ligand X^-. The terminal Cr–Cl bond lengths were set at 2.32 Å. The bridging M–X distances in the symmetrical geometry were set at 1.1 times a typical Cr–X distance (Cr–F = 1.90, Cr–Cl = 2.32, Cr–I = 2.75 Å). Simulation of a poorer σ donor in a nonbridging ligand position was achieved by increasing the relevant chlorine atom exponents to 2.100. This resulted in a decrease in metal–ligand overlaps. (Variation of the H_{ii} values did not always produce the expected change in energy of the "z^2" orbital on the metal center in a standard octahedral complex. We will comment on this effect elsewhere.) For the carboxylate system at the symmetrical geometry Cr–O = 2.2 Å, C–O = 1.24 Å, C–C = 1.55 Å, and C–H = 1.00 Å. For the $Cr_2(CO)_{10}H^-$ system, all C–M–C angles were put at either 90 or 180°, and Cr–C = 1.90 Å, C–O = 1.14 Å, C–O = 1.14 Å, and Cr–Cr = 3.38 Å.

For the outer-sphere case the $Cr_2Cl_{12}^{7-}$ "complex" was used as a model system. The bond length change between oxidant and reductant was 0.02 Å for the two axial bonds in **32**. Cf. similar changes in ref 5. The separation of the two metal atoms was 8.6 Å, and therefore the distance between the two interacting peripheral Cl atoms is 3.76 Å. The Na^+ ion or H_2O molecule was inserted symmetrically between these two atoms.

Registry No. $Cr_2Cl_{11}^{6-}$, 67113-72-8.

References and Notes

(1) On leave from the Chemistry Department, University of Newcastle-on-Tyne, Newcastle-on-Tyne, NE1 7RU, England. Present address: Chemistry Department, University of Chicago, Chicago Ill. 60637.
(2) (a) H. Taube, "Electron Transfer Reactions of Complex Ions in Solution", Academic Press, New York, N.Y., 1970; (b) A. G. Sykes, *Adv. Inorg. Chem. Radiochem.*, **10**, 153 (1967); (c) R. G. Wilkins, "The Study of Kinetics and Mechanism of Reactions of Transition Metal Complexes", Allyn and Bacon, Boston, Mass., 1974; (d) R. G. Linck, *MTP Int. Rev. Sci.: Inorg. Chem., Ser. One*, **9** (1972); (e) R. G. Linck, *MTP Int. Rev. Sci.: Inorg. Chem., Ser. Two*, **9** (1974); (f) M. L. Tobe, "Inorganic Reaction Mechanisms", Nelson, London, 1972; (g) F. Basolo and R. G. Pearson, "Mechanisms of Inorganic Reactions", Wiley, New York, N.Y., 1967; (h) W. L. Reynolds and R. W. Lumry, "Mechanisms of Electron Transfer", Ronald Press, New York, N.Y., 1966; (i) J. Halpern, *Q. Rev., Chem. Soc.*, **15**, 207 (1961); (j) N. Sutin, *Annu. Rev. Phys. Chem.*, **17**, 119 (1966).
(3) (a) W. F. Libby, *J. Phys. Chem.*, **56**, 863 (1952); (b) R. J. Marcus, B. J. Zwolinski, and H. Eyring, *ibid.*, **58**, 432 (1954); *Chem. Rev.*, **55**, 157 (1955); (c) R. A. Marcus, *J. Chem. Phys.*, **24**, 966 (1956); **26**, 867, 872 (1957); (d) R. A. Marcus, *Discuss. Faraday Soc.*, **29**, 21 (1960); (e) R. A. Marcus, *J. Phys. Chem.*, **67**, 853 (1963); (f) R. A. Marcus, *J. Chem. Phys.*, **43**, 679 (1965); (g) R. A. Marcus, *J. Phys. Chem.*, **72**, 891 (1968); (h) N. S. Hush, *Trans. Faraday Soc.*, **57**, 557 (1961); (i) P. P. Schmidt, *Electrochemistry*, **5** (1975).
(4) In the ferri- and ferrocyanide ions, however, the Fe–C bond length is shorter in the reduced Fe^{II} (low-spin d^6) species than in the oxidized Fe^{III} (low-spin d^5) species. Here the set of t_{2g} orbitals are Fe–C bonding due to the strong π-acceptor nature of the CN^- ligand. The nature of the orbital containing the transferred electron may not be the only factor affecting the M–L bond length. See ref 5.
(5) N. J. Hair and J. K. Beattie, *Inorg. Chem.*, **16**, 245 (1977).
(6) Throughout this paper we shall follow current practice and use the terminology $M^{II} \equiv M^{II}(H_2O)_6^{2+}$, $M^{II}Cl = M^{II}(H_2O)_5Cl^+$, etc.
(7) J. A. Jafri, G. Worry, M. D. Newton, N. Sutin, and R. A. Marcus, Abstracts, 173rd National Meeting of the American Chemical Society, New Orleans, La., Mar 1977, No. PHYS 210.
(8) The lanthanide and actinide ions in solution probably have coordination numbers greater than 6.
(9) J. Halpern and L. E. Orgel, *Discuss. Faraday Soc.*, **29**, 32 (1960).
(10) H. Taube and E. S. Gould, *Acc. Chem. Res.*, **2**, 321 (1969).
(11) For some EHMO calculations on reactions occurring at electrode surfaces see C.-N. Lai and A. T. Hubbard, *Inorg. Chem.*, **13**, 1199 (1974).
(12) L. E. Orgel, Report 10eme Conseil Chimique, Solvay, Bruxelles, 1956.
(13) The frontier orbitals of this fragment are available in A. R. Rossi and R. Hoffmann, *Inorg. Chem.*, **14**, 365 (1975).
(14) The sorts of ligands which can act as bridging groups in these inner-sphere reactions need to have an accessible pair of electrons after coordination. Thus pyridine is never found as a bridging ligand. NH_3 is also never seen in a bridging position, but coordinated CH_3 has been shown to act as a transferable bridge (H. L. Fritz, J. H. Espenson, D. A. Williams, and G. A. Molander, *J. Am. Chem. Soc.*, **96**, 2378 (1974)). Halide ions are ideally suited as bridges and the relative rates of reaction of halide-bridged systems we will use diagnostically later.
(15) (a) J. D. Dunitz and L. E. Orgel, *J. Chem. Soc.*, 2594 (1953). (b) The assumption in (a) concerning the linear nature of the $[(NH_3)_5Co]_2O_2^{4+}$ species also treated in this paper is incorrect. W. P. Schaefer and R. E. Marsh, *J. Am. Chem. Soc.*, **88**, 178 (1966), show that the O_2 unit is tilted relative to the Co–Co axis. (c) W. Wojciechowski and B. Jezowska-Trzebiatowska in "Theory and Structure of Complex Compounds", B. Jezowska-Trzebiatowska, Ed., Pergamon Press, London, 1964. (d) J. Glerup, *Acta Chem. Scand.*, **26**, 3775 (1972). (e) R. J. H. Clarke, M. L. Franks, and P. C. Turtle, *J. Am. Chem. Soc.*, **99**, 2473 (1977). (f) J. S. Filippo, P. J. Fagan, and F. J. DiSalvo, *Inorg. Chem.*, **16**, 1016 (1977).
(16) The behavior of the π-type orbitals on asymmetrization for ligands other than our simple halide ions may well be different due, among other things, to different geometrical requirements of the ligand bridge. [For example, XYZ^- (N_3^-, NCS^-, SCN^-) ligands coordinate such that the MXY angle is much less than 180°.] Calculations with a bridging azide group indicate that for some π^n configurations the surface is very soft or even a small stabilization of the asymmetric structure is observed.
(17) (a) R. Hoffmann, *Acc. Chem. Res.*, **4**, 1 (1971); (b) P. J. Hay, J. C. Thibeault, and R. Hoffmann, *J. Am. Chem. Soc.*, **97**, 4884 (1975).
(18) For a discussion of these fluoride structures see R. D. Peacock, *Adv. Fluorine Chem.*, **7**, 113 (1973).
(19) (a) J. E. Earley and T. Fealey, *Chem. Commun.*, 331 (1971). (b) P. M. Smith, T. Fealey, J. E. Earley, and J. V. Silverton, *Inorg. Chem.*, **10**, 1943 (1971). (c) An early molecular orbital study of this ion exists: C. K. Jørgensen and L. E. Orgel, *Mol. Phys.*, **4**, 215 (1961).
(20) (a) The structures of several of these species with different counterions are described by D. J. Hodgson, *Prog. Inorg. Chem.*, **19**, 173 (1975). (b) E. I. Stiefel, *ibid.*, **22**, 1 (1977).
(21) J. C. Morrow, *Acta Crystallogr.*, **15**, 857 (1962).
(22) R. F. Ziolo, R. H. Stanford, G. R. Russmann, and H. B. Gray, *J. Am. Chem. Soc.*, **96**, 7910 (1974).
(23) A. M. Mathieson, D. P. Mellor, and N. C. Stephenson, *Acta Crystallogr.*, **5**, 185 (1952).

(24) (a) M. Ciechanowicz and A. C. Skapski, *J. Chem. Soc. A*, 1792 (1971); (b) R. J. D. Gee and H. M. Powell, *ibid.*, 1795 (1971).
(25) H. Preut, W. Wolfes, and H.-J. Haupt, *Z. Anorg. Allg. Chem.*, **412**, 121 (1975).
(26) N. G. Vannerberg, *Acta Chem. Scand.*, **17**, 79 (1963).
(27) See for example H. Fischer, G. M. Tom, and H. Taube, *J. Am. Chem. Soc.*, **98**, 5512 (1976).
(28) (a) R. D. Wilson, S. A. Graham, and R. Bau, *J. Organomet. Chem.*, **91**, C49 (1975); (b) R. A. Love, H. B. Chin, T. F. Koetzle, S. W. Kirtley, B. R. Whittlesey, and R. Bau, *J. Am. Chem. Soc.*, **98**, 4491 (1976); (c) J. Roziere, J. M. Williams, R. P. Stewart, J. L. Petersen, and L. F. Dahl, *ibid.*, **99**, 4497 (1977).
(29) L. B. Handy, J. K. Ruff, and L. F. Dahl, *J. Am. Chem. Soc.*, **92**, 7237 (1970).
(30) In the case of the carbonyl hydride molecules an analysis of the temperature dependence of the vibrational spectrum shows a very soft (and anharmonic) surface for movement of the H atom: private communication with D. F. Schriver, Northwestern University.
(31) H. Steinfink and J. H. Burns, *Acta Crystallorgr.*, **17**, 823 (1964).
(32) For the classification of mixed-valence species and an exhaustive description of known examples see M. B. Robin and P. Day, *Adv. Inorg. Chem. Radiochem.*, **10**, 247 (1967).
(33) T. D. Ryan and R. E. Rundle, *J. Am. Chem. Soc.*, **83**, 2814 (1961).
(34) M. B. Robin, *Inorg. Chem.*, **1**, 337 (1962).
(35) (a) H. W. Richardson, J. R. Wasson, and W. E. Hatfield, *Inorg. Chem.*, **16**, 484 (1977); (b) R. C. E. Belford, D. E. Fenton, and M. R. Truter, *J. Chem. Soc., Dalton Trans.*, 17 (1974); (c) H. W. Richardson and W. E. Hatfield, *J. Am. Chem. Soc.*, **98**, 835 (1976).
(36) (a) For a review of these structures see K. S. Murray, *Coord. Chem. Rev.*, **12**, 1 (1974). (b) R. G. Wollmann and D. N. Hendrickson, *Inorg. Chem.*, **16**, 723 (1977). (c) H. Lüken, J. W. Buchler, and K. L. Lay, *Z. Naturforsch., B*, **31**, 1596 (1976).
(37) (a) D. Baumann, H. Endres, H.-J. Keller, and J. Weiss, *J. Chem. Soc., Chem. Commun.*, 853 (1973); (b) D. Baumann, H. Endres, H.-J. Keller, B. Nuber, and J. Weiss, *Acta Crystallogr., Sect. B*, **31**, 40 (1975).
(38) (a) R. S. Mulliken, *J. Chim. Phys. Phys.-Chim. Biol.*, **61**, 20 (1964). (b) The related case of photochemical electron transfer has been considered by G. Ramunni and L. Salem, *Z. Phys. Chem. (Frankfurt am Main)*, **101**, 123 (1976).
(39) Computing the energetics of the complete reaction surface is certainly not a useful procedure with our semiempirical molecular orbital method.
(40) With $Cr^{III}(H_2O)_5X$: (a) H. Taube and H. Meyers, *J. Am. Chem. Soc.*, **76**, 2103 (1954); (b) H. Taube, H. Meyers, and R. L. Rich, *ibid.*, **75**, 4118 (1953); (c) H. Taube and E. L. King, *ibid.*, **76**, 4053 (1954); (d) D. L. Ball and E. L. King, *ibid.*, **80**, 1091 (1958); (e) J. P. Birk and J. H. Espenson, *ibid.*, **90**, 2266 (1968); (f) R. Snellgrove and E. L. King, *Inorg. Chem.*, **3**, 288 (1964).
(41) With $Cr^{III}(NH_3)_5X$: (a) A. E. Ogard and H. Taube, *J. Am. Chem. Soc.*, **80**, 1084 (1958); (b) J. P. Candlin, J. Halpern, and D. L. Trimm, *ibid.*, **86**, 1019 (1964).
(42) (a) H. Diebler, P. H. Dodel, and H. Taube, *Inorg. Chem.*, **5**, 1688 (1966); (b) D. L. Toppen and R. G. Linck, *ibid.*, **10**, 2635 (1971).
(43) J. P. Candlin, J. Halpern, and S. Nakamura, *J. Am. Chem. Soc.*, **85**, 2517 (1963).
(44) (a) J. P. Candlin and J. Halpern, *Inorg. Chem.*, **4**, 766 (1965); (b) M. C. Moore and R. N. Keller, *ibid.*, **10**, 747 (1971).
(45) C. K. Jørgensen, "Modern Aspects of Ligand Field Theory", North-Holland Publishing Co., Amsterdam, 1971.
(46) R. C. Patel, R. E. Ball, J. F. Endicott, and R. G. Hughes, *Inorg. Chem.*, **9**, 23 (1970).
(47) (a) J. Halpern and J. Rabani, *J. Am. Chem. Soc.*, **88**, 699 (1966); (b) G. Navon and G. Stein, *J. Phys. Chem.*, **69**, 1391 (1965).
(48) (a) W. R. Mason, *Coord. Chem. Rev.*, **7**, 241 (1972). (b) W. R. Mason, E. R. Berger, and R. C. Johnson, *Inorg. Chem.*, **6**, 248 (1967). (c) From our discussion above the symmetrically bridged intermediate postulated for this system in ref 2g cannot be correct.
(49) (a) J. Halpern and J. P. Maher, *J. Am. Chem. Soc.*, **86**, 2311 (1964); **87**, 5361 (1965); (b) G. N. Schrauzer, E. Deutsch, and R. J. Windgassen, *ibid.*, **90**, 2441 (1968); (c) P. B. Chock, R. B. K. Dewar, J. Halpern, and L.-Y. Wong, *ibid.*, **91**, 82 (1969).
(50) (a) J. A. Silverman and R. W. Dodson, *J. Phys. Chem.*, **56**, 846 (1952); (b) D. Bunn, F. S. Dainton, and S. Duckworth, *Trans Faraday Soc.*, **57**, 1131 (1961); (c) J. Hudis and A. C. Wahl, *J. Am. Chem. Soc.*, **75**, 4153 (1953).
(51) (a) N. Sutin, J. K. Rowley, and R. W. Dodson, *J. Phys. Chem.*, **65**, 1248 (1961); (b) R. J. Campion, T. J. Conocchioli, and N. Sutin, *J. Am. Chem. Soc.*, **86**, 4591 (1964).
(52) (a) N. Sutin, *Acc. Chem. Res.*, **1**, 225 (1968); (b) T. W. Newton and F. B. Baker, *Inorg. Chem.*, **3**, 569 (1964); (c) J. H. Espenson, *ibid.*, **4**, 1533 (1965).
(53) (a) J. P. Birk, *Inorg. Chem.*, **9**, 125 (1970); (b) J. P. Birk, *J. Am. Chem. Soc.*, **91**, 3189 (1969).
(54) An earlier claim that atom transfer was not complete in some inner-sphere reductions of $IrCl_6^{2-}$ by Cr^{II} is probably due to some competition from the outer sphere route: R. N. F. Thorneley and A. G. Sykes, *Chem. Commun.*, 331 (1969).
(55) J. H. Espenson and R. J. Christensen, *J. Am. Chem. Soc.*, **91**, 7311 (1969).
(56) (a) D. Seewald, N. Sutin, and K. O. Watkins, *J. Am. Chem. Soc.*, **91**, 7307 (1969); (b) W. G. Movius and R. G. Linck, *ibid.*, **92**, 2677 (1970); (c) J. A. Stritar and H. Taube, *Inorg. Chem.*, **8**, 2281 (1969).
(57) J. H. Espenson, *Inorg. Chem.*, **4**, 1533 (1965).
(58) B. Grossman and A. Haim, *J. Am. Chem. Soc.*, **92**, 4835 (1970).
(59) A. Haim and W. K. Wilmarth, *J. Am. Chem. Soc.*, **83**, 509 (1961).
(60) J. H. Espenson, *Inorg. Chem.*, **4**, 1025 (1965).
(61) (a) T. J. Meyer and H. Taube, *Inorg. Chem.*, **7**, 2369 (1968); (b) R. G. Yalman, *ibid.*, **1**, 16 (1962).
(62) This relationship has not been emphasized before to our knowledge.
(63) J. H. Espenson, *Inorg. Chem.*, **4**, 121 (1965).
(64) "Intermediates" are also observed[56c] for V^{II} and Eu^{II} reductions of $Ru^{III}(carbox)(NH_3)_5$ systems. Here, however, this "intermediate" is identical in both redox systems and is probably the $Ru^{II}(carbox)(NH_3)_5^+$ species, i.e., not a binuclear intermediate. This arises since the V^{II} is certainly of the outer-sphere type and the Eu^{III} system is very labile.
(65) (a) G. Gordon, *Inorg. Chem.*, **2**, 1277 (1963); (b) J. C. Sullivan, *J. Am. Chem. Soc.*, **84**, 4256 (1962).
(66) D. W. Carlyle and J. H. Espenson, *J. Am. Chem. Soc.*, **91**, 599 (1969).
(67) (a) J. P. Candlin, J. Halpern, and D. L. Trimm, *J. Am. Chem. Soc.*, **86**, 1019 (1964); (b) J. H. Espenson, *Inorg. Chem.*, **4**, 121 (1965).
(68) (a) R. T. Wang and J. H. Espenson, *J. Am. Chem. Soc.*, **93**, 380 (1971); (b) A. Ekstrom, A. B. McLaren, and L. E. Smythe, *Inorg. Chem.*, **16**, 1032 (1977).
(69) (a) H. Diebler and H. Taube, *Inorg. Chem.*, **4**, 1029 (1965); (b) T. J. Conocchioli, G. H. Nancollas, and N. Sutin, *J. Am. Chem. Soc.*, **86**, 1453 (1964); (c) A. Haim and N. Sutin, *ibid.*, **88**, 5343 (1966).
(70) R. D. Cannon and J. Gardiner, *J. Am. Chem. Soc.*, **92**, 3800 (1970).
(71) O. J. Parker and J. H. Espenson, *J. Am. Chem. Soc.*, **91**, 1968 (1969).
(72) K. Shaw and J. H. Espenson, *J. Am. Chem. Soc.*, **90**, 6622 (1968).
(73) H. J. Price and H. Taube, *Inorg. Chem.*, **7**, 1 (1968).
(74) (a) F. Nordmeyer and H. Taube, *J. Am. Chem. Soc.*, **90**, 1162 (1968); (b) R. G. Gaunder and H. Taube, *Inorg. Chem.*, **9**, 2627 (1970).
(75) (a) E. S. Gould, *J. Am. Chem. Soc.*, **94**, 4360 (1972); (b) E. R. Dockal, E. T. Everhart, and E. S. Gould, *ibid.*, **93**, 5661 (1971); (c) H. Spiecker and K. Wieghardt, *Inorg. Chem.*, **16**, 1290 (1977).
(76) See for example R. J. Balahura, *J. Am. Chem. Soc.*, **98**, 1487 (1976).
(77) J. E. Earley, *Prog. Inorg. Chem.*, **13**, 243 (1970).
(78) C. Bifano and R. G. Linck, *Inorg. Chem.*, **7**, 980 (1968); *J. Am. Chem. Soc.*, **89**, 3945 (1967).
(79) J. K. Burdett, *Inorg. Chem.*, **14**, 375 (1975).
(80) J. R. Perumareddi, *Coord. Chem. Rev.*, **4**, 73 (1969).
(81) J. Glerup, O. Mønsted, and C. E. Schäffer, *Inorg. Chem.*, **15**, 1399 (1976).
(82) (a) R. D. Cannon and J. E. Earley, *J. Am. Chem. Soc.*, **88**, 1872 (1966); (b) A. Haim and N. Sutin, *ibid.*, **88**, 434 (1966); (c) D. E. Pennington and A. Haim, *Inorg. Chem.*, **5**, 1887 (1966); (d) J. M. DeChant and J. B. Hunt, *J. Am. Chem. Soc.*, **89**, 5988 (1967); **90**, 3695 (1968).
(83) T. J. Williams and C. S. Garner, *Inorg. Chem.*, **9**, 2058 (1970).
(84) D. E. Pennington and A. Haim, *Inorg. Chem.*, **6**, 2138 (1967).
(85) P. Benson and A. Haim, *J. Am. Chem. Soc.*, **87**, 3826 (1965).
(86) See the discussion in ref 2d.
(87) D. Gaswick and A. Haim, *J. Am. Chem. Soc.*, **96**, 7845 (1974).
(88) (a) P. H. Dodel and H. Taube, *Z. Phys. Chem. (Frankfurt am Main)*, **44**, 92 (1965); (b) J. Doyle and A. G. Sykes, *J. Chem. Soc. A*, 795 (1967); (c) A. Zwickel and H. Taube, *J. Am. Chem. Soc.*, **83**, 793 (1961); (d) J. C. Sheppard and A. C. Wahl, *ibid.*, **79**, 1020 (1957); (e) L. Gjertsen and A. C. Wahl, *ibid.*, **81**, 1572 (1959); (f) M. Shporer, G. Ron, A. Loewenstein, and G. Navon, *Inorg. Chem.*, **4**, 362 (1965).
(89) The effect of the solvent here in pushing apart these two surfaces is reminiscent of a similar effect in the photochemically accessible surfaces in ethylene: L. Salem and W.-D. Stohrer, *J. Chem. Soc., Chem. Commun.*, 140 (1975).
(90) (a) H. C. Stynes and J. A. Ibers, *Inorg. Chem.*, **10**, 2304 (1971); (b) R. A. Marcus in "Dahlem Workshop on the Nature of Seawater", 1976, p 477.
(91) R. Farina and R. G. Wilkins, *Inorg. Chem.*, **7**, 514 (1968).
(92) Marcus[90b] has suggested a preequilibrium between high- and low-spin Co^{III} to rationalize the observed rate constant. By use of an equilibrium constant of 10^{-5}, the observed rates may be fitted quite well. However, we calculated earlier an energy difference between the two forms of $\sim 8 \times 10^3$ cm^{-1} which leads to an equilibrium constant of $\sim 10^{-17}$. With this equilibrium constant the rate is fitted very poorly indeed.
(93) A. Holstein, *Ann. Phys. (N.Y.)*, **8**, 3, 25 (1959).
(94) E. N. Economou, K. L. Ngai, and T. L. Reinecke in "Linear and Non-Linear Electron Transport in Solids", J. T. Devreese and V. E. Van Doren, Ed., Plenum Press, New York, N.Y., 1975.
(95) (a) R. Hoffmann, *J. Chem. Phys.*, **39**, 1397 (1963); (b) R. Hoffmann and W. N. Lipscomb, *ibid.*, **36**, 2179, 3489 (1962); **37**, 2872 (1962).